Science of the Total Environment 939 (2024) 173144

Contents lists available at ScienceDirect

Science of the Total Environment

journal homepage: www.elsevier.com/locate/scitotenv

Review

A review on mathematical modeling of microbial and plant induced permafrost carbon feedback

Niloofar Fasaeiyan [a,1], Sophie Jung [a,1], Richard Boudreault [a], Lukas U. Arenson [b], Pooneh Maghoul [a,*]

[a] Sustainable Infrastructure and Geoengineering Lab (SIGLab), Department of Civil, Geological and Mining Engineering, Polytechnique Montreal, Montreal, QC, Canada
[b] BGC Engineering Inc., Vancouver, BC, Canada

HIGHLIGHTS

- Assessing microbial activity's crucial role in permafrost carbon feedback;
- Emphasizing the need for enhanced tools to precisely forecast carbon fluxes during permafrost thaw;
- Highlighting the complex nature of permafrost ecosystems, influenced by various geophysical factors;
- Recognizing the extensive use of process-based models in simulating greenhouse gas production, movement, and release;
- Encouraging integrated models for understanding permafrost dynamics in the face of climate change using thermo-hydro-biogeochemical processes.

GRAPHICAL ABSTRACT

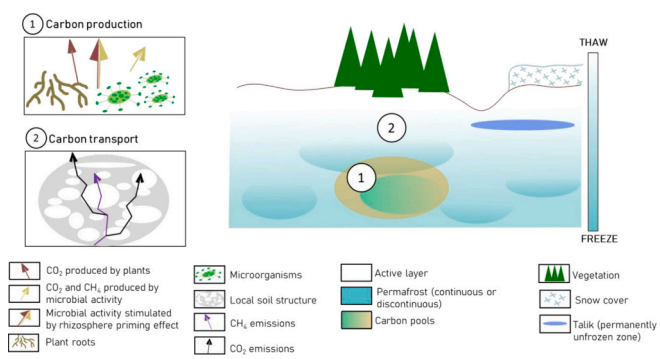

ARTICLE INFO

Editor: Sergey Shabala

Keywords:
Permafrost carbon feedback (PCF)
Biogenic activity
Microbial activity
Climate change
Mathematical model
Plant-microbe interaction

ABSTRACT

This review paper analyses the significance of microbial activity in permafrost carbon feedback (PCF) and emphasizes the necessity for enhanced modeling tools to appropriately predict carbon fluxes associated with permafrost thaw. Beginning with an overview of experimental findings, both in situ and laboratory, it stresses the key role of microbes and plants in PCF. The research investigates several modeling techniques, starting with current models of soil respiration and plant-microorganism interactions built outside of the context of permafrost, and then moving on to specific models dedicated to PCF. The review of the current literature reveals the complex nature of permafrost ecosystems, where various geophysical factors have considerable effects on greenhouse gas emissions. Soil properties, plant types, and time scales all contribute to carbon dynamics. Process-based models are widely used for simulating greenhouse gas production, transport, and emissions. While these models are beneficial at capturing soil respiration complexity, adjusting them to the unique constraints of permafrost environments often calls for novel process descriptions for proper representation. Understanding the temporal coherence and time delays between surface soil respiration and subsurface carbon production, which are controlled by numerous parameters such as soil texture, water content, and temperature, remains a challenge. This review highlights the need for comprehensive models that integrate thermo-hydro-biogeochemical

* Corresponding author.
E-mail address: pooneh.maghoul@polymtl.ca (P. Maghoul).
[1] Equal contribution, First co-author.

https://doi.org/10.1016/j.scitotenv.2024.173144
Received 8 January 2024; Received in revised form 11 March 2024; Accepted 9 May 2024
Available online 18 May 2024
0048-9697/© 2024 The Authors. Published by Elsevier B.V. This is an open access article under the CC BY-NC-ND license (http://creativecommons.org/licenses/by-nc-nd/4.0/).

processes to understand permafrost system dynamics in the context of changing climatic circumstances. Furthermore, it emphasizes the need for rigorous validation procedures to reduce model complexity biases.

1. Introduction

Permafrost, defined as ground that remains below zero degree Celsius for at least two consecutive years, stands as a critical component of Earth's system. The top layer of a permafrost site, called the active layer, undergoes seasonal freeze-thaw cycles. The thickness of the active layer depends on local and climate conditions such as vegetation, soil composition, air temperature, solar radiation, snow cover, and wind regimes (Liu et al., 2019). Climate warming has adversely affected permafrost regions, resulting in accelerated thawing and increase active layer thicknesses (Liu et al., 2023; Rossi et al., 2022; Gruber, 2020; Duchesne et al., 2015).

Permafrost is currently estimated to represent the largest source of terrestrial carbon sink (Hugelius et al., 2020; Froese et al., 2008; Schuur and Abbott, 2011). Permafrost thaw, however, could lead tothe release of vast amounts of embedded greenhouse gases into the atmosphere, subsequently exacerbating climate change and further permafrost thaw. The permafrost carbon pool includes organic carbon stored within the top 3 meters of the ground, carbon in deposits deeper than 3 meters, and permafrost carbon that formed on land during the ice ages but is now found on shallow submarine shelves in the Arctic. Near surface permafrost soils which corresponds to the soil layer located between 0 and 3 meters deep, contain about 1 035 ± 150 Pg carbon (where 1 Pg = 1 billion tons) (Charles Tarnocai et al., 2009; Hugelius et al., 2014; Schuur et al., 2015). This amount is of significant importance considering that 2 050 Pg carbon is stored in the near-surface soil layer (top 3 m) of the rest of Earth's biomass, excluding the Arctic and boreal regions. This means that, based on current understanding, 33% of the global carbon pool is actually stored in the permafrost region which only represents 15% of the total global soil area (Schuur et al., 2015). Mishra et al. (2021) validated the estimate of near-surface permafrost carbon, confirming approximately 1 014 Pg with an updated database (Mishra et al., 2021). However, this likely represents a conservative minimum, as permafrost carbon extends beyond 3 m depth, suggesting a larger portion of global soil carbon is stored in permafrost.

The degradation of permafrost due to climate warming impacts the net carbon balance in the ecosystem, as well as other processes such as vegetation growth and death, biogenic activities, and subsequently, emissions of greenhouse gases such as methane (CH_4) and carbon dioxide (CO_2) into the atmosphere, which are the main drivers of global warming (McGuire et al., 2018; Shogren et al., 2019; Vonk et al., 2019). Greenhouse gas emissions from permafrost are already estimated at between 0.3 and 0.6 billion tons of carbon each year, roughly equivalent to 7 % of the world's total carbon emissions from burning coal, oil and natural gas (Homer-Dixon and Froese, 2021; Schuur, 2019). By considering only gradual and top-down thaw, cumulative permafrost emissions could reach 150 billion tons of carbon by the year 2100 without aggressive climate policies or climate change adaptation strategies. This amount is nearly half the world's remaining carbon budget if we want to keep global warming under 2 °C, which is the limit set in international climate agreements (Homer-Dixon and Froese, 2021). It is worth noting that carbon emissions from permafrost thaw are not even fully accounted for in global emissions budgets or in recently updated national commitments for emission cuts made under the Paris Agreement. This process, which is called positive carbon feedback, can shift the permafrost from a sink of carbon to a source. This has been already observed in many different permafrost sites like the Arctic tundra (Koven et al., 2013; Lawrence et al., 2012; Schuur et al., 2013; Slater and Lawrence, 2013; Hollesen et al., 2011).

For over 15 years, numerous studies have been conducted to develop mathematical models to predict the potential release of carbon from permafrost due to global warming and assess its impact on the rate of climate change. Different considerations have been made to refine the mathematical models and improve the precision of permafrost carbon decomposition predictions. For instance, the freeze/thaw state of the active layer was incorporated into the models (Lawrence et al., 2008; Koven et al., 2011). Another model improvement involved assessing the counterbalancing effect of plant carbon uptake, which can partially mitigate permafrost carbon release while also contributing to the accumulation of new soil carbon (Qian et al., 2010). Based on projections from these models and under the assumption of the current trajectory of climate warming (Representative Concentration Pathway RCP 8.5), the permafrost region could release between 5 and 15 % of the total permafrost carbon pool by the year 2100 (Schuur et al., 2022). Moreover, it is anticipated that the emission of carbon from thawing permafrost will have long-lasting consequences on the global climate. On average, these models project that about 59% of the total permafrost carbon emissions will take place beyond the year 2100 (Schuur et al., 2015). Estimating carbon releases over such extended time frames is challenging and becomes even more complex as it requires accounting for the inertia of a warming climate, which leads to the thawing of near-surface permafrost and cascading changes in the ecosystems that result in the release of greenhouse gases. Over the past few years, the biogeochemical scientific community has done tremendous work to identify and isolate key factors in soil respiration to incorporate into their mathematical models. Progress in microbial ecology has led to an improved understanding of the processes driving microbial decomposition, allowing for the development of increasingly complex carbon feedback models (Todd-Brown et al., 2012).

In this review paper, we aim to review existing mathematical models for PCF from microbial and plant activities. Particular attention will be paid to models which have already been applied to permafrost. Further, we will discuss how the soil respiration models developed for different soil types can be adapted to thawing permafrost specificity. The paper begins by providing key features for understanding the impact of climate change on permafrost. It then describes the methodology employed to collect the data required to develop this study. This is followed by a comprehensive systematic review of the role of microbial communities in PCF and the most important influencing factors. The last two sections are devoted to the description of mathematical models built to account for soil carbon feedback, not limited to the permafrost context to begin with, followed by models that incorporate the complexities specific to permafrost. Finally, we offer some perspectives on identified research gaps and future model advancements.

2. Climate change and permafrost thaw

According to Canada's Changing Climate Report (2023) (Lulham et al., 2023), in the Arctic regions, temperatures have been warming at approximately four times the rate as the average global warming, a phenomenon known as Arctic amplification. The Arctic regions are located in the northern circumpolar region of the Earth. This area includes the tundra biome and parts of the boreal biome, which are characterized by areas such as continuous and discontinuous permafrost zones and persistent winter snow cover. By examining air temperatures (2 m above ground surface) between 1981 and 2020 and comparing this trend to changes in sea ice concentration and sea surface temperature, Isaksen et al. (2022) found that the warming rate for the Northern Barents Sea, located in the Arctic Ocean corresponds to 5 to 7 times the global warming averages. Changes in air temperature and sea ice are the main indicators of the environmental transformation and changes in hydrological and ecological processes in permafrost regions (Vaks et al.,

2020; Wang et al., 2020).

Permafrost temperature is linked to ground surface temperature, which, in turn, is directly influenced by fluctuations in air temperature as well as shifts in snow cover, surface hydrology, and vegetation dynamics. Consequently, the pace of permafrost warming exhibits variations across the Arctic landscape, contingent upon dynamic, local environmental conditions. The implications of permafrost carbon reservoirs for global climate hinge on the dynamics of permafrost thaw and the extent to which this carbon will be released into the atmosphere as greenhouse gases. According to a recent assessment by Palmtag et al. (2022), nearly half of the Soil Organic Carbon (SOC) in the northern circumpolar permafrost region is situated in the top meter of the soil, rendering it particularly susceptible to the effects of climate change. It is essential to be able to predict the timing of this release and the degree to which it could be offset by an increase in plant biomass.

A study by Berner et al. (2020) has shown that between 1985 and 2016, tundra greenness (greening) increased by nearly 37 % of sample sites and decreased (browning) by nearly 5 % of sample sites. From these data, they concluded that in recent decades, summer warming has boosted plant productivity in much, but not all, of the Arctic tundra biome. This is an important phenomenon to be considered since the greening of permafrost regions will increase soil respiration, which is a key ecosystem process that releases carbon from the soil in the form of CO_2 (Mahecha et al., 2010). In fact, soil respiration refers to the production of carbon dioxide when soil organisms breathe. It is commonly divided into autotrophic and heterotrophic respiration, which correspond to the emission of CO_2 from plant and root respiration, and microorganisms, respectively. Besides CO_2 emissions from soil respiration, microorganisms called methanogens produce methane as a metabolic byproduct in hypoxic conditions. The two entities (plants and microorganisms) do not only exist independently of each other but live in symbiosis so that the dynamics of one influence those of the other. For instance, the vegetation process affects microbial activity and the accumulation of soil biomass. Plants affect the availability of soil nutrients and subsequently the local microbial activity. This is why the results published by Berner et al. (2020) raise concerns and encourage further research on the greening of permafrost regions caused by climate change. However, there are currently substantial uncertainties regarding the effects of vegetation on the carbon cycle in permafrost, and whether rates of carbon accumulation exceed the release of greenhouse gases at a local scale (Koven et al., 2015; McGuire et al., 2012).

The complexity of understanding the effect of climate change on the permafrost ecosystem, as depicted in Fig. 1, arises from the fact that permafrost thaw triggers repercussions across interlinked dimensions of the ecosystem. These ramifications include vegetation growth, microbial activity, and soil water content. The more global warming intensifies, the more permafrost thaw threatens global warming. The conversion of ground ice into water facilitates expedited soil thawing through convective heat transfer from flowing water (Magnin and Josnin, 2021). This process, accelerated by factors like wildfires (Kuklina et al., 2022; Li et al., 2021; Holloway et al., 2020), leads to an accelerated ground collapse, giving rise to structures known as thermokarsts or retrogressive thaw slumps (Runge et al., 2022; Lewkowicz and Way, 2019; Segal et al., 2016). As these formations emerge, they not only expose deeper permafrost layers to rapid thawing but also induce changes in local hydrology. This alteration in hydrology establishes an accelerated feedback loop on thaw due to convective heat transfer. Following the ground collapse, the heat permeates into deeper soil layers, as substantiated by recorded temperatures from various long-term monitoring sites in the circumpolar permafrost region of the northern hemisphere (Biskaborn et al., 2019). This evidence underscores that the temperature increase affects the entire ground profile.

The active layer, where most vegetation and microorganisms reside, is the permafrost segment most susceptible to climate change. Rising summer temperatures and duration result in the active layer's expansion as degrading permafrost extends its depth. This expansion increases the thickness of the active layer, which significantly affects the types of vegetation that can thrive in the permafrost region. Plant roots are constrained by the active layer's thickness, preventing them from penetrating deeper. Consequently, the thickening of the active layer induces changes in the metabolic respiration pathway and modifies the fluxes of CO_2 and CH_4 (Frolking et al., 2011).

3. Methodology

The search strategy employed for data collection and the literature review presented in this paper was as follows: data was collected from ISI Web of science with different combinations of keywords. The paper search was limited to papers in English and the search for keywords was

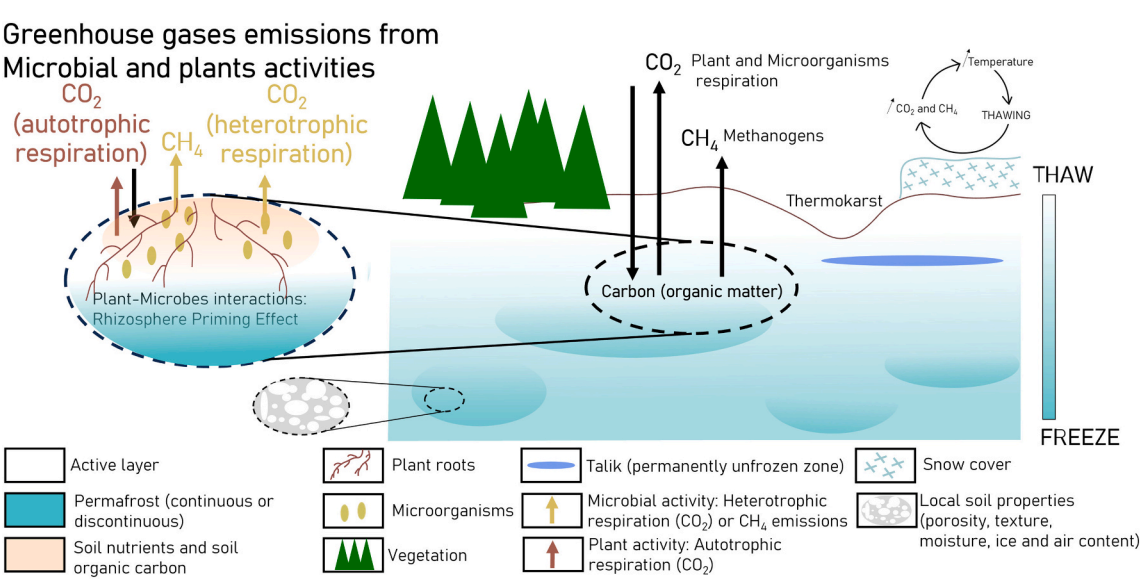

Fig. 1. Illustrating the intricacies of the permafrost ecosystem, with a specific focus on the carbon cycle. Permafrost, acting as a significant carbon reservoir, actively influences global carbon dynamics. This figure highlights the dual role of vegetation in carbon input to the soil and the contribution of plants and microbial activity to CO_2 and CH_4 emissions. The carbon feedback process is influenced by factors such as vegetation type, thermokarst presence, snow cover, and local soil properties. The thermal flux and hydraulic flow, affected by these factors, play a crucial role in the production and transport of carbon back to the atmosphere.

done within the titles, abstracts, and author keywords. The number of papers found for each search is given in Table 1.

The objective of this review paper is to provide an overview of the existing mathematical models for predicting PCF resulting from global warming, and more specifically, existing models to account for the greenhouse gas emissions related to microbial activity coupled with vegetation growth in permafrost regions.

The scientific community's attention has recently been directed explicitly to the subject of permafrost, and in particular to the quantity of carbon stored in these frozen soil layers that may be released into the atmosphere due to climate change. Over the last several years, an increasing number of scientists have begun to warn about permafrost thawing and the ramifications that this could have in terms of increased carbon emissions and thus aggravating global warming. Since 2015, one can notice a remarkable increase in the number of publications per year, with 30 papers published in 2015 and over 50 papers published in 2021. Among the first 633 papers found with the keywords *Permafrost* and *Carbon feedback*, only 7.6 % of them specifically dealt with the microbial activity in permafrost.

As our primary focus revolves around reviewing mathematical models describing PCF related to microbial activity, we conducted a search using the keywords *Permafrost*, *Carbon feedback*, and *Microbial activity*. Among the 48 papers identified, 25 were pertinent to our goal of reviewing the literature concerning the influence of permafrost thaw on microbial activity. These selected papers are subsequently detailed in Section 4.

Subsequently, we added the keyword *Model* to the search in order to find papers describing the mathematical model of the processes by which microbes contribute to PCF. This research returned sixteen papers. Among those sixteen papers, only two of them proposed a model of greenhouse gas emissions related to microbial activity in thawing permafrost. The keyword *Model* appeared in all these abstracts, albeit without proposing a model themselves, indicating that they helped lay the foundations for future modeling attempts.

As few papers were found proposing mathematical models of carbon emission related to the activity of microorganisms in permafrost, we also took an interest in existing work related to the modeling of soil respiration. Under the keywords *Soil respiration*, *Carbon feedback*, and *Mathematical model*, we found 15 papers. Analyzing the papers, we noted that about 90 % of them are analytical, experimental studies, and field measurements for specific sites and two of them presented a formulation to estimate the soil respiration (CO_2 emission from the soil surface) (Burke et al., 2017; Luke and Cox, 2011). Because these key phrases did not provide the expected results, we conducted a modified search using the keywords *Modeling*, *Soil* CO_2, and *Production*, and *Transport* which has been led to finding 401 papers. To identify the works among these 401 papers, which focused on developing numerical models for greenhouse gas emission from the soil, we first selected the articles based on their titles and abstracts to eliminate research that did not focus on mathematical modeling. The remaining articles were thoroughly evaluated by reading the entire contents. Through evaluating the full text, we identified the works that proposed innovative mathematical models or significantly improved existing models related to microbial activity and its relationship to greenhouse gas emissions in permafrost regions. Priority was given to studies that offered new parameters and processes or gave enhanced insights into basic knowledge. To avoid repetition and redundancy, papers that presented trivial differences from previously reviewed models were excluded. Reviewing the existing literature revealed a research gap in mathematical models addressing the interaction of microbes, plants, and soil. So, in the next step, we upgraded the search strategy once again to search for papers related to plant-microbes interaction known as Rhizosphere priming effect (RPE). Using *Rhizosphere priming effect* and *Modeling* keywords, we found 81 papers. Since the primary concern of this study is on the mathematical modeling of the biogeochemical processes contributing to greenhouse gas emission from permafrost, the articles regarding the modeling of RPE were chosen by thoroughly reviewing their entire content.

Table 1
Keywords for the search strategy.

Keywords	Number of publications
Permafrost & Carbon feedback & Microbial activity	48
Permafrost & Carbon feedback & Microbial activity & Model	16
Soil respiration & Carbon feedback & Mathematical model	15
Modeling & Soil CO_2 & Production & Transport	401
Rhizosphere priming effect & Modeling	81

4. Role of microbial communities in PCF

Microbial communities, which include bacteria, archaea, and fungi, have been facing radical changes in their living conditions due to climate change. These changes have caused alteration in microbial metabolic activity and potentially create a positive feedback loop from permafrost (Schuur et al., 2008). In order to accurately model greenhouse gas emissions resulting from microbial activity in permafrost soils, it is crucial to comprehend the processes that connect the dynamics of microbial communities to the breakdown of carbon at various temperatures spanning from sub-zero to warmer conditions (Nikrad et al., 2016; Reyes and Lougheed, 2015). Nevertheless, modeling carbon feedback from permafrost microbial activity is challenging because as temperatures rise, permafrost thaws, and this triggers a complicated interplay of various processes. Research has shown that comprehending microbial processes in permafrost thaw necessitates an understanding of the impacts of a multitude of physical variables. These variables include soil temperature, moisture levels, structure of soil pore network, chemical composition, as well as considerations of temporal and spatial scales.

The diagram in Fig. 2 describes the process by which the rise in temperature initiates permafrost thaw, setting off a series of subprocesses that ultimately culminate in increasing microbial activity, subsequently increasing greenhouse gas emissions. When permafrost thaws, it adds moisture to the soil and releases trapped substances like minerals, organic matter, and nutrients from the frozen ground. This, in turn, stimulates microbial activity and facilitates vegetation growth. As a result, processes like methanogenesis, which produces methane without oxygen, and both heterotrophic and autotrophic respiration, get a boost and cause more greenhouse gases to be released. Nevertheless, the situation is more complex, given that additional competing mechanisms also play a role in the overall process of greenhouse gas emissions. For example, the impact of vegetation on microbial activity can be either positive or negative. Vegetation functions as thermal insulation on the ground surface, which alters the energy balance and creates a favorable environment for microbial activity. It can offer nutrients that promote microbial growth. However, conversely, vegetation can also exert a detrimental impact on microbial activity by depleting essential nutrients required for microbial community development.

The complex process of greenhouse gas emission is governed by a combination of various factors, such as temperature (both atmospheric and soil temperatures), vegetation type, soil moisture (including precipitation levels and water flow from ground ice melt), pore water salinity, soil characteristics (quantity and elemental composition of the substrate), and the structure of the microbial community (abundance, activity, and types of microorganisms). Table 4 in appendix provides an overview of the diverse research scopes explored within the recently published articles concerning carbon emissions associated with microbial activity in permafrost.

4.1. Effect of temperature and soil water content on microbial activity

One of the most complex phenomena in permafrost dynamics is soil

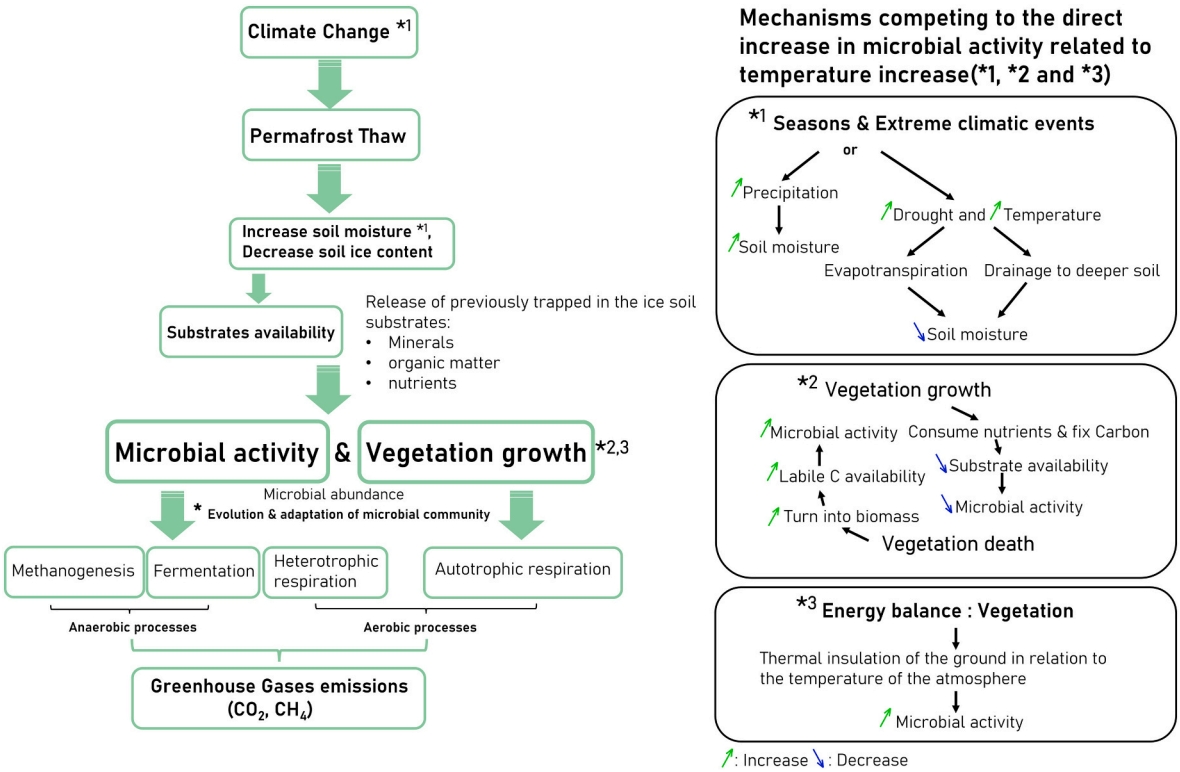

Fig. 2. Schematic representation of the various mechanisms that drive an increase in greenhouse gas emissions as a result of climate change. The rise in temperature initiates permafrost thaw, setting off a series of processes that ultimately culminate in increasing microbial activity, effectively increasing greenhouse gas emissions. However, it's important to note that these processes are not linear, meaning that not everything exhibits a simple positive or negative correlation. Various competing mechanisms come into play in the context of PCF.

respiration during freeze/thaw cycles. Several studies reveal a rapid increase, up to 10 times bigger, in CO_2 effluxes as soils shift from frozen to unfrozen states (Elberling and Brandt, 2003). A common way to measure microbial processes or directly CO_2 effluxes sensitivity to temperature is through the Q_{10} parameter. This parameter is used to quantify the effect of a 10-degree increase in temperature on any processes through the ratio $(T + 10^{\circ}C)/T$, where T is the standard reference temperature (Nottingham et al., 2019). For example, Elberling and Brandt (2003) demonstrated that the Q_{10} value for CO_2 effluxes is higher when assessed based on the change in CO_2 effluxes as temperature increases from negative values to 0 °C compared to temperatures above 0 °C (e.g., $Q_{10}(T < 0^{\circ}) = 21.7$ and $Q_{10}(T > 0^{\circ}) = 2.0$ (Elberling and Brandt, 2003)). This reveals that the impact of temperature on CO_2 effluxes is non-linear, emphasizing the need for comprehensive studies to gain a deeper understanding of this phenomenon.

Beyond the effect of freeze/thaw changes, the soil water content also plays an important role in microbial respiration, which was investigated by Schädel et al. (2016). In their research, they did not confine their investigation solely to the impact of a 10-degree rise in soil temperature but they also examined the consequences of transitioning from aerobic to anaerobic conditions. Aerobic soil conditions refer to soil with ample oxygen availability, whereas anaerobic soil conditions relate to soil characterized by limited to no oxygen content, typically associated with waterlogged or flooded soil. They worked on 25 soil incubation studies from the permafrost zone including different ecosystems (boreal forest, peatland and tundra). They showed that increasing temperature by 10 °C (from 5 to 15 °C) resulted in an increase in carbon release by a factor of 2. Furthermore, they demonstrated that when the same temperature increase was coupled with alterations in soil moisture levels (corresponding to moving from aerobic to anaerobic soil conditions), there was a 3.4-fold greater release of carbon in aerobic conditions compared to anaerobic conditions. Song et al. (2020) also published a work suggesting that more carbon is released under aerobic conditions compared to anaerobic conditions.

Monson et al. (2006) conducted a field experiment for six years, wherein they measured the net ecosystem carbon dioxide exchange in a subalpine forest situated within the Rocky Mountains. In their study, they demonstrated that the high sensitivity of soil respiration rates to temperature changes can be attributed to a soil microbial community characterized by exponential growth and rapid substrate utilization. Their findings revealed that not only the kinetics of microorganisms change with rising temperatures, but the composition of soil microbial communities also varies between snow-covered periods and summer. The researchers observed that microbes collected from beneath the snow cover exhibited exponential growth even at 0 °C, with their growth rate significantly accelerating as temperatures increased. The respiration rates increased by orders of magnitude when the soil temperature rose from −1 °C to 0 °C. This phenomenon can be attributed to the phase change of ice into liquid water, which enhances substrate diffusion within the soil and facilitates nutrient accessibility for microorganisms, as explained by Stapel et al. (2016). As such, these findings raise several key factors to be taken into account when studying the role of microbial communities in PCF. Soil water content is for example a crucial factor to be considered, given its complex relationship with various mechanisms. Climate change not only alters the frequency of freeze/thaw cycles but also leads to extreme droughts and intense precipitation events. These changes in soil moisture have profound implications for microorganisms, as they rely on it for essential functions such as motility, feeding, and reproduction. However, the study provided by Meisner et al. (2021) shows the complexity of the effect of soil water content on microbial activity. They have shown that freeze/thaw and drying/rewetting cycles have slightly different impacts on microbial community structure and microbial activity. Their study revealed that drying/rewetting cycles exert stronger effects on soil microbial communities and CO_2 production

compared to freeze/thaw cycles. This discrepancy can be attributed to the more gradual change in soil moisture during freeze/thaw cycles, allowing soil microorganisms more time to adapt to the altered osmotic pressure. Additionally, the magnitude and form of carbon production are regulated by moisture conditions and the associated availability of oxygen.

Taken together, these findings highlight the importance of investigating the variation of soil water content, in the form of:

- freeze/thaw cycles
- drying/rewetting cycles
- aerobic/anaerobic conditions

as it plays a critical role in shaping microbial communities, carbon dynamics, and the overall functioning of ecosystems.

4.2. Temporal and spatial considerations

Among the different physical parameters involved, *time* is another crucial aspect to be considered, given that numerous mechanisms evolve over time. Various processes, including water diffusion across different soil layers, the evolution of microorganism communities, plant growth, canopy phenology, and seasonal temperature variations, exhibit temporal dynamics that significantly influence the overall system behavior. Recognizing the temporal dimension is essential for comprehensively understanding the complex interplay of these mechanisms and their cumulative effects (Knoblauch et al., 2021; Yun et al., 2022; Qin et al., 2021; Peng et al., 2020; Bouskill et al., 2020; Yang et al., 2018; Schneider von Deimling et al., 2015). For instance, it has been observed that short-term experiments tend to overestimate carbon feedback due to their failure to capture the non-linear, long-term dynamics occurring within the soil layers, including vegetation growth, soil organic matter content, and nutrient transformations, as highlighted by Bouskill et al. (2020). The complex response of the ecosystem to time is further exemplified by the interaction between plants and microorganisms. Hicks Pries et al. (2013) investigated the response of autotrophic and heterotrophic respiration to permafrost thaw. They divided ecosystem respiration into two components for autotrophic respiration (above and below plant structures) and two components for heterotrophic respiration (young and old soil). Their findings revealed that permafrost thaw leads to an increase in both autotrophic and heterotrophic respiration. Initially, autotrophic respiration accounts for a larger portion of ecosystem respiration (40 % to 70 %) as plants grow and become more active. However, as the newly formed plant biomass decomposes and transforms into labile carbon, the heterotrophic microbial respiration in the active layer and permafrost eventually outpaces autotrophic respiration, turning the active layer into a significant source of CO_2. Additionally, Schneider Von Deimling et al. (2015) demonstrated through their numerical simulations that the highest methane emission rates occur once thermokarst lakes reach their maximum extent and when abrupt thawing under these lakes is taken into account. This time-dependent phenomenon cannot be fully captured in short-term experiments. Another time-dependent factor that cannot be adequately demonstrated in short-term experiments is the alteration in microbial taxa. Monteux et al. (2020) emphasized that increasing temperatures, in addition to enhancing microbial activity, can facilitate the colonization of microorganisms by different microbial taxa, such as those from the overlying active layer. This process can have significant implications for global greenhouse gas emissions.

The *spatial* dimension plays also a significant role in governing the interactions and processes occurring within permafrost ecosystems, as numerous mechanisms are contingent upon the specificities of the local environment. Factors such as soil properties (porosity, tortuosity), land covers, microbial communities, and even the presence of localized features like thermokarst lakes or suprapermafrost taliks can exhibit substantial spatial variations. The permafrost region exhibits various land covers including forests, tundra, wetlands, barren areas, and bedrock (Palmtag et al., 2022). These diverse land cover types establish distinct conditions influencing the thermal and hydraulic characteristics of the local permafrost being studied. This geographical variability underscores the need for region-specific analyses and emphasizes the importance of considering local conditions and characteristics when studying the effects of global warming on permafrost ecosystems (Torre Jorgenson et al., 2001).

In reality, the various mechanisms involved in permafrost carbon dynamics do not operate independently, but all the different parameters interact. The fate of carbon stored in permafrost, whether it is released as methane or carbon dioxide, depends on which mechanism predominates. The carbon balance of a given location, determining whether it acts as a carbon sink or source, depends on the complex relationship between microorganism activity and vegetation activity. This complex equilibrium cannot be simply attributed to competition for soil nutrients. Indeed, Sturm et al. (2005) have shown that an increase in shrub abundance leads to an increase in snow depth, which in turn promotes higher soil temperatures in winter, greater microbial activity, and more plant-available nitrogen (N). These factors, in turn, benefit the growth of shrubs during the following summer. However, this balance can be disrupted over time due to changes in dominant mechanisms, which may arise from specific events such as thermokarst formation or extreme climate events. This highlights the dynamic nature of the system and the potential for shifts in the underlying processes that govern carbon dynamics in permafrost ecosystems.

5. Mathematical models for soil carbon feedback

The response of terrestrial ecosystems to global warming, whether they amplify or mitigate it, depends on various processes that impact the carbon cycle in these ecosystems. To account for the global carbon exchange between soils and the atmosphere, different models known as Earth system models (ESMs) have been developed over the past few years. Earth system models incorporate a broad range of components, such as the atmosphere, oceans, land, ice, and their interactions in order to represent the carbon cycle at the global scale. Land surface models (LSMs) are implemented into the global ESMs to account for the different mechanisms at stake at a given time and space scale. LSMs focus on simulating and representing the physical and biophysical processes occurring at or near the Earth's land surface, with a particular emphasis on land-based components such as soil, vegetation, and hydrology, along with their interactions with the atmosphere. LSMs capture processes like energy exchange, water balance, vegetation dynamics, nutrient cycling, and land-atmosphere interactions. They are typically employed at a detailed spatial resolution and are commonly used for regional or local-scale studies. The primary objective of LSMs is to provide a comprehensive understanding of land surface processes and their influences on climate, weather patterns, and ecosystem dynamics. They serve as vital components within larger Earth system models, supplying essential information on land-related variables to the broader system.

In the context of this review paper, as mentioned above, we are interested in the different models and the related mathematical framework that aim to quantify the contribution of microbial activity and vegetation to PCF. Different types of LSMs vary in their mathematical formulations and approaches, as follows:

- **Physics-based models**: Physics-based models rely on physical laws and equations to simulate land surface processes. These models use principles from physics, such as mass conservation, heat transfer, and fluid dynamics to describe and simulate the behavior of the ecosystem. Physics-based models aim to capture the physical processes and interactions with a high level of detail and accuracy.
- **Process-based models**: Process-based models combine both physical laws with observed mechanisms to provide a mechanistic

understanding of land surface processes. These models are typically based on scientific understanding and empirical data and aim to capture the fundamental processes of energy balance, water balance, vegetation dynamics, nutrient cycling, and land-atmosphere interactions.

- **Empirical/statistical models**: Empirical or statistical models, as the name implies, are based on observed data and statistical relationships. These models use historical data or observations to develop statistical relationships between input variables and the output of interest. They may use regression analysis, machine learning algorithms, or statistical techniques to establish relationships and make predictions. Empirical models are often used when detailed physical or mechanistic understanding is not available or when a large amount of observed data is accessible.

These categories are not mutually exclusive, and many LSMs incorporate elements from different approaches. For instance, process-based models combine physics-based formulations for key processes with empirical relationships for specific variables or parameters. The choice of the type of LSM depends on the research objectives, available data, computational resources, and the level of detail and accuracy required for the specific application.

Different LSMs have their own strengths and limitations, and researchers select the most appropriate model based on the specific research question and available resources. When it comes to modeling PCF, we have already discussed in Section 4 the need to take into account the effect of global warming on permafrost regions and different factors affecting the complex processes involved. McGuire et al. (n.d.) have compared 13 different process-based models that simulated the permafrost region carbon dynamics between 1960 and 2009 in order to assess what factors explain the variability in the sensitivity of permafrost carbon pools among the models. The diverse models produced very different outcomes when assessing carbon exchange between permafrost soil and the atmosphere. This disparity highlights the need for continued efforts to gain a thorough understanding of the underlying processes governing carbon fluxes in permafrost soils.

The following two sections present a comprehensive review of the various mathematical frameworks present in the literature, which aim to capture the mechanisms responsible for carbon emissions associated with microbial activity in permafrost degradation. Starting with models that were originally designed for any soil type and are not specifically aimed at permafrost, followed by a focus on models developed for permafrost specifically.

5.1. Mathematical models for soil respiration

Various biological processes referred to as soil respiration account for the production of CO_2 in the soil, which is eventually released into the atmosphere. In this section, we provide a review of mathematical models that have been developed to simulate soil respiration. As mentioned in the methodology section, we have included in our bibliography models, CO_2 emissions from microorganism activity, although these models have not been specifically developed for permafrost soils. By considering a wide range of models, we aim to provide a comprehensive overview of the existing mathematical frameworks that have been employed to study processes of carbon feedback from soil ecosystems to the atmosphere. So, by discussing CO_2 emissions, we are first focusing on soil respiration. We noticed that soil respiration models are commonly divided into two main components. The first component focuses on the production of carbon dioxide, while the second component deals with the transport of this CO_2 through various soil layers, ultimately leading to its release into the atmosphere. In the transport mechanisms, CO_2 is either transported in its gaseous phase or dissolved CO_2 in soil's liquid phase, whether the process of CO_2 dissolution is explicitly modeled or not. Regarding the production terms, soil respiration, as mentioned previously, is further classified into two types: autotrophic respiration, which refers to plant and root respiration, and heterotrophic respiration, which refers to microorganism respiration. In reality, not all of the carbon contained in soil is released as CO_2, but some of it is converted to methane by metabolic processes involving microbes called methanogens. The fate of this methane varies depending on the specific reactions that occur during its transport from the soil to the atmosphere. Ultimately, this methane can be released into the atmosphere as methane itself or as carbon dioxide if it has been oxidized before being emitted.

On one hand, soil CO_2 production originates from plant-related factors, including root growth respiration and root maintenance respiration. On the other hand, microorganisms contribute to CO_2 production through the decomposition of plant litter and the breakdown of soil organic matter (SOM), particularly associated with older plant litter (Pendall et al., 2003). In the overlap between plant and microorganism processes, there is another mechanism involving both, known as the *rhizosphere priming effect*. This process occurs when microorganisms living in close proximity to plant roots utilize and metabolize organic materials found in rhizome deposits. This organic matter can include dead plant material, root exudates, decomposed residues, and microbial biomass. Rhizome deposits are organic material or biomass that accumulates around the rhizomes of plants over time, while rhizomes are living structures that play a vital role in plant growth, propagation, and nutrient storage. They are horizontal, underground stems of plants from which roots can grow. As rhizomes grow and spread, they interact with the surrounding soil and contribute to the accumulation of organic matter.

In our analysis of mathematical models that characterize GHG emissions from microorganisms and plants, we choose to begin with Šimůnek and Suarez (1993) particular model due to its one-dimensional nature, which facilitates an initial understanding of the problem at hand. Šimůnek and Suarez (1993) developed a process-based model to describe CO_2 production and transport in soil. The model is one-dimensional and incorporates CO_2 production, CO_2 transport with water flow and heat flux in a porous unsaturated medium. As such, the model can be divided into four main components: CO_2 production, CO_2 transport, water flow, and heat flux.

CO_2 production (S) is attributed to microbial respiration and plant root respiration. The total CO_2 production is the sum of these two components:

$$S = \gamma_m + \gamma_r \tag{1}$$

in which γ_m $\left[L^3\ L^{-3}\ T^{-1}\right]$ is the production of CO_2 by soil microorganisms and γ_r $\left[L^3\ L^{-3}\ T^{-1}\right]$ is the CO_2 production by soil plant roots. The model assumes that CO_2 production deviates from its optimal rate, which is considered to occur at 20 °C under optimal water and solute concentrations. Thus the CO_2 production rate is defined as the sum of the optimal CO_2 production rate by microbes (γ_{m0}) and the optimal CO_2 production rate by plant roots which are respectively multiplied by six reduction functions. The reduction functions are introduced in order to account for the effects of depth, pressure head, osmotic head, temperature, CO_2 concentration, and time on CO_2 production by microbes and plant roots. The mathematical framework is the same for both plant and microorganisms CO_2 production, which is why we are providing a detailed structure only for γ_m as follows:

$$\gamma_m = \gamma_{m0} f(z) f(h) f(T) f(c_a) f(h_\phi) f(t) \tag{2}$$

in which.

- $f(z)$ $[L^{-1}]$ is the Depth Dependence factor: Microbial respiration decreases with depth due to decreasing root mass and available organic matter. Plant root CO_2 production depends on a root growth function and a depth-dependent root distribution function, which have been determined to account for the water uptake by plant roots.

- $f(h)$ [−] is the Pressure Head and Osmotic Head Dependence factor: Microbes' CO_2 production is influenced by soil water content. The model assumes maximum microbial respiration occurs at a soil water pressure head of 0.01–1 MPa. Two threshold values are considered to account for reduced microbial respiration at high and low-pressure heads. The decrease at high pressure head is due to decreased availability of free water, while at low pressure head, oxygen becomes unavailable due to high water content.
- $f(T)$ [−] is the Temperature Dependence factor: Both microbial and plant root CO_2 production are assumed to be affected by temperature following the Arrhenius law:

$$f(T) = exp\left(\frac{E}{RT}\frac{T - T_{20}}{T_{20}}\right) \tag{3}$$

where E [L^2 T^{-1}] is the activation energy of the reaction, T [K] is the absolute temperature and R [M L^2 T^{-2} K^{-1} n^{-1}] is the universal gas constant. The optimal CO_2 production rate occurs at 20 °C.

- $f(c_a)$ [−] is the CO_2 Concentration Dependence factor: The production rate of CO_2 is related to its own concentration or similarly to oxygen deficiency as soil CO_2 and O_2 concentrations (c_a and c_{O_2}) are assumed to be related by $c_a = 0.21 - c_{O_2}$ (Šimůnek and Suarez, 1993). $f(c_a)$ is given by the Michaelis-Menten equation that describes the reaction rate as function of a substrate concentration in this case it's the production rate of CO_2 as function of CO_2 or O_2 concentration. The general form of the Michaelis-Menten equation is:

$$V = \frac{V_{max}[S]}{K_m + [S]} \tag{4}$$

where V [L^3 L^{-3} T^{-1}] is the reaction rate, V_{max} [L^3 L^{-3} T^{-1}] is the maximum reaction rate, $[S]$ [ML^{-3}] is the substrate concentration, and K_m [ML^{-3}] is the Michaelis constant, indicating the substrate concentration at which the reaction rate is half of V_{max}. Reduction functions for CO_2 production are the same for microbes and plant roots.

- $f(t)$ [−] is the Time Dependence factor: The time-dependent reduction function accounts for changes in CO_2 production related to different growth stages of plants. Note that the temperature reduction function already describes the diurnal variation in CO_2 production and that other reduction functions already cover dependence on seasonal dynamics.

Finally, CO_2 production is integrated throughout the soil profile.

CO_2 transport in the soil is modeled using multiphase Fick's law.

$$\frac{\partial C_T}{\partial t} = -\frac{\partial}{\partial z}(J_{da} + J_{dw} + J_{ca} + J_{cw}) - Q_{c_w} + S \tag{5}$$

Diffusion and convection are the two mechanisms considered for CO_2 transport in both the liquid and gas phases of the soil porous medium. J_{da} [L T^{-1}] and J_{dw} [LT^{-1}] are the coefficients of diffusion, respectively, in the gas phase and liquid phase. J_{ca} [L T^{-1}] and J_{cw} [L T^{-1}] are the coefficients of convection, respectively, in the gas phase and the liquid phase. Q_{c_w} [T^{-1}] is a sink term accounting for the dissolved CO_2 removed from the soil by root water uptake and S is an additional production/sink term. It is worth noting that diffusion accounts for the movement from an area of higher concentration to an area of lower concentration while convection accounts for transport related to water and air flow. In their model, Simunek and Suares consider the dissolved CO_2 that is removed from the soil by root water uptake, but they ignore the interaction of dissolved CO_2 with the solid phase. In the water phase, both convection and dispersion are considered, while in the gas phase, diffusion is assumed to be dominant, and convection is neglected. The diffusion coefficients are assumed to be temperature-dependent. The parameters are obtained from known material parameters or the resolution of the water flow equation.

One-dimensional **Water flux** in an unsaturated medium is calculated using Richard's equation, in which the effect of temperature is neglected:

$$\frac{\partial \theta_w}{\partial t} = \frac{\partial}{\partial z}\left[K\left(\frac{\partial h}{\partial z} - 1\right)\right] - Q \tag{6}$$

in which θ_w [L^3 L^{-3}] the volumetric water content, K [L T^{-1}] the unsaturated hydraulic conductivity and h the pressure head. In this model Q [L^3 L^{-3} T^{-1}] is a sink term developed to account for plant root water uptake, which is the volume of water removed from a volume of soil per unit of time. Similarly, as the framework used to describe CO_2 production, water uptake is described as the amount of water absorbed by the plant's roots, taking into account the reduction from the maximum amount of water that the roots could potentially absorb within their root zone. They considered two reduction functions that are related to osmotic stress response and water stress response, respectively. The two functions have the same form; however, the empirical parameters have different values. Osmotic stress refers to the adaptive mechanisms that plants employ to maintain osmotic balance during periods of imbalanced solute concentrations. As such osmotic stress is a specific type of water stress related to imbalances in solute concentrations, water stress is a broader term encompassing the overall effects of limited water availability on plants. Ultimately, plant water uptake depends on root vegetation growth. The model under consideration incorporates a formulation for vegetation growth that is both time and temperature dependent.

The **heat flux** is calculated by considering both conduction and heat transported by flowing water:

$$C\frac{\partial T}{\partial t} = \frac{\partial}{\partial z}\left[\lambda(\theta_w)\frac{\partial T}{\partial z}\right] - C_w\frac{\partial q_w T}{\partial z} \tag{7}$$

where C [J L^{-3} K^{-1}] and C_w [J L^{-3} K^{-1}] are the volumetric heat capacities of porous medium and liquid phase, respectively. $\lambda(\theta_w)$ [W L^{-1} K^{-1}] is the coefficient of the soil apparent thermal conductivity and q_w [L T^{-1}] is the soil water flux. The volumetric heat capacity of the porous medium is the sum of contributions from the solid phase, organic matter, liquid phase, and gas phase. The resulting soil temperature is used in solving the CO_2 transport equation.

Fang and Moncrieff (1999) have also built a one-dimensional, process-based model with the same global framework as Šimůnek and Suarez (1993) namely by describing the CO_2 production and transport in a one-dimensional porous unsaturated medium. Despite their similar mathematical framework, Fang and Moncrieff have provided a more detailed process to account for the CO_2 production. More particularly they have further detailed the dependence of soil respiration on soil water content and soil oxygen concentration. Oxygen is an environmental factor, which has an influence on respiration rates of plant tissues. It has been shown that at low O_2 concentrations, the respiration rate linearly increases with the oxygen concentration. The increase slows down to a maximum for high O_2 concentrations. Assuming that oxygen concentration has the same effect on microbial respiration, the dependence of soil respiration rate on ambient oxygen concentration can be described by the Michaelis-Menten equation (Eq. (4)) (Fang and Moncrieff, 1999).

In their model, CO_2 production is divided into the root and microbes contributions. First, the calculation of heterotrophic respiration, denoted as R_m [L^2 T^{-1}], is based on the effective quantity of decomposing material, which corresponds to soil organic matter. To represent microbial respiration adequately, two distinct rates of decomposition are taken into account. This approach considers both the decomposition of labile carbon and the more resistant fraction, often referred to as slow soil organic carbon:

$$R_m = \alpha \frac{dM}{dt} = \gamma_m \left[\lambda M + \frac{k_{ris}}{k_{lab}} (1-\lambda) M \right] \tag{8}$$

in which α [M M^{-1}] is a coefficient representing the amount of CO_2 produced from the decomposition per unit of dry organic matter, M [M L^{-2}] is the amount of effective decomposing organic matter, γ_m [L^2T^{-1}] is the heterotrophic respiration rate, k_{lab} [M M^{-1} T^{-1}] is the decomposition rates for labile organic matter, k_{ris} [M M^{-1} T^{-1}] is the decomposition rates for resistant organic matter, and λ [M M^{-1}] is the ratio of labile to total amount of organic matter. All the carbon is assumed to be produced as CO_2.

Second, the autotrophic respiration, denoted as R_r $\left[L^2\ T^{-1}\right]$, is associated with two factors: the rate at which roots breathe and the quantity of root biomass in the soil. Regarding root respiration, they have assumed that a linear relationship can be established between the respiration rate and the root biomass for each particular root size class:

$$R_r = \gamma r \sum \frac{\gamma_{ri}}{\gamma_r} B_i \tag{9}$$

where γ_r $\left[L^{-2}\ T^{-1}\right]$ is the autotrophic respiration rate, γ_{ri} $\left[L^{-2}\ T^{-1}\right]$ is the respiration rate parameter of root size class i and B_i $\left[M\ L^{-2}\right]$ is the root biomass of size class i. By acknowledging that the rates of respiration in roots per unit of dry mass differ based on root diameter or size class, they established a direct correlation between root biomass and respiration rate for each specific root size class.

The total CO_2 production is the sum of heterotrophic and autotrophic respiration integrated along the soil profile to account for the depth dependence of both respiration. Besides, they have accounted for the influence of environmental factors on the respiration rates in a similar manner as (Šimůnek and Suarez, 1993), which consists of expressing autotrophic (γ_r) and heterotrophic (γ_m) respiration rates, as a deviation from the optimal respiration rates, γ_{r0} and γ_{m0}. As such, they have multiplied the optimal respiration rates by three scaling functions to account for the dependence of soil respiration on temperature, water content, and O_2 concentration in the soil. The three scaling functions are the same for both heterotrophic and autotrophic respiration functions:

- **Temperature dependence**: The temperature dependence is treated similarly as (Šimůnek and Suarez, 1993) with the Arrhenius law (Eq. (3)).
- **Soil moisture dependence**: The soil systems are assumed to possess a natural respiratory potential that depends on soil moisture content. However, this potential remains unrealized when the soil is dry. When water is added to the soil, soil respiration increases, but the rate of increase gradually decreases as soil moisture further increases.
- **Soil oxygen concentration dependence**: Similar to (Šimůnek and Suarez, 1993), soil respiration rate is assumed to depend on soil oxygen concentration according to the Michaelis-Menten equation (Eq. (4)). The equation describes that respiration rates first increase linearly with increasing O_2 concentration until a given O_2 concentration, followed by a decrease in respiration rate for further increase in O_2 concentration.

CO_2 transport is treated with the same framework as in (Šimůnek and Suarez, 1993). They have considered both gaseous diffusion and liquid phase dispersion. In contrast to Simunek and Suares' proposed model, Fang and Moncrieff's (1999) model disregarded the aspects of liquid phase diffusion and the transport mechanisms related to root water uptake.

Jassal et al. (2004) also proposed a process-based model. The mathematical framework of their model is very similar to Fang and Moncrieff (1999) and Šimůnek and Suarez (1993). Again this one-dimensional model incorporates CO_2 production and CO_2 transport while considering the water flow and heat flux in a porous unsaturated medium. The model proposed considers both heterotrophic and autotrophic respiration as sources of carbon dioxide production in the soil, in line with other existing models. Their approach stands out from the others due to its consideration of the variability in the quantity and distribution of organic matter within the soil profile. To address this, they model the soil as a multi-layered system, acknowledging the distinct organic matter characteristics across different layers. The organic matter content varies with soil depths, with specific amounts allocated to each layer. Consequently, each layer is divided into two subpools: labile carbon C_{soilL} $\left[M\ L^{-3}\right]$, representing easy to decompose and reactive organic compounds that microorganisms can readily utilize for energy production, and resistant carbon C_{soilR} $\left[M\ L^{-3}\right]$, comprising more challenging-to-decompose carbon compounds. 3 % of the total soil organic matter is assumed to represent the portion of labile carbon, while 45 % is considered as resistant carbon. The remaining portion is categorized as passive carbon, meaning that it does not contribute to CO_2 production.

CO_2 production from microbial respiration is separately calculated for each pool as two reaction terms with two specific rate constants, k_L $\left[T^{-1}\right]$ and k_R $\left[T^{-1}\right]$, related to the decomposition of labile and resistant carbon, respectively. The overall CO_2 production from heterotrophic respiration is as follows:

$$R_{CS} = k_L C_{soilL} + k_R C_{soilR} \tag{10}$$

As mentioned above, labile organic matter, known for its easy decomposition, acts as a readily accessible carbon source that is rapidly decomposed by soil microbes. On the other hand, resistant organic matter is less susceptible to microbial degradation, resulting in a slower decomposition rate. In a similar vein as in Fang and Moncrieff's model, the estimation of carbon dioxide production resulting from autotrophic respiration depends on root size. They consider two classes: fine and coarse roots. The calculation involves multiplying the products of the respective rate constants and root mass density for each class in the following manner:

$$R_{CR} = k_{F_{root}} M_{F_{root}} + k_{C_{root}} M_{C_{root}} \tag{11}$$

where $M_{F_{root}}$ $\left[ML^{-3}\right]$ and $M_{C_{root}}$ $\left[M\ L^{-3}\right]$ represent the carbon mass densities of fine and coarse roots, respectively, while $k_{F_{root}}$ $\left[T^{-1}\right]$ and $k_{C_{root}}$ $\left[T^{-1}\right]$ stand for the corresponding respiration rate constants. To determine the total carbon dioxide production in the soil profile, they sum R_{CR} $\left[ML^{-3}\ T^{-3}\right]$ and R_{CS} $\left[M\ L^{-3}\ T^{-3}\right]$ in all layers multiplied by scaling factors. The scaling factors are defined to account for the influence of temperature and soil moisture. The temperature scaling factor is defined based on Q_{10} coefficient, which represents the relative increase in respiration rate for a $10^{\circ}C$ temperature increase:

$$\alpha(T) = Q_{10}^{\left(\frac{T-T_{ref}}{10}\right)} \tag{12}$$

The soil moisture scaling factor, as CO_2 production decreases at both very low and very high soil water contents, is defined as a piece-wise linear function of relative water-filled porosity as represented in Fig. 3.

The **CO_2 transport** in the soil is modeled by diffusion in both the gaseous and liquid phases. They also took into account CO_2 uptake by plant roots associated with root water uptake.

The model is then calibrated against in situ measurements. The CO_2 concentration measurements were done on easy-to-access soil during three 1-week rainless periods in August, October, and December 2000. The soil temperatures, soil CO_2 concentration, and soil water contents obtained from numerical modeling were then compared to the respective field observations. In situ measurements show that soil CO_2 production and efflux are correlated with soil temperature, which is accordingly reproduced by the model. The variation in soil temperature is quite well reproduced by the model. The variation in soil water con-

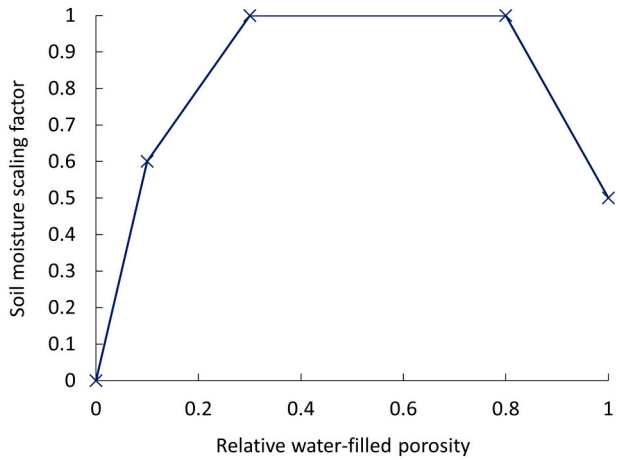

Fig. 3. Scaling of CO_2 production with soil moisture scaling factor defined as a piece-wise linear function of relative water-filled porosity based on (Jassal et al., 2004).

tent, on the other hand, seems to deviate from in situ measurements. Following the rain on October 3rd and 19th, the soil water content, within the first few centimeters of the soil, increased by 1 %, which resulted in a considerable increase in observed soil CO_2 concentration. The most likely explanation for this increase seems to be a rapid change in soil microbial activity resulting from a slight increase in soil water content during a rain event, which the model could not accurately simulate. The presence of 'bypass flow' in macropores, like old dead root canals, made it challenging to match the modeled and actual soil water levels after rain events. This discrepancy reveals a significant difference between the measured soil CO_2 emissions and soil moisture levels at shallow soil depths and the expected values. Furthermore, starting from December 11th, the measured soil CO_2 concentration and soil water contents at a 2 cm depth were found to be lower than the values predicted by the model. This variation is attributed to the occurrence of freezing within the top few centimeters at the soil surface, as the air temperature drops below −1 °C. This freezing effect, which has a direct effect on soil water content, is not taken into account in their model. The model does not account for the CO_2 uptake by photosynthesis. However, the measurements show that this hypothesis had no significant effect on the modeled CO_2 efflux compared to the measured value. This is probably due to the vegetation distribution and low light levels on the forest floor, which limited the photosynthetic uptake of CO_2 during the daytime.

Samuels-Crow et al. (2018) developed a process-based model to simulate soil CO_2 production and transport. This model bases itself on the work of Fang and Moncrieff (1999). Besides, the model is assessed by comparing its results to the environmental field observations obtained for a single growing season.

CO_2 production occurs as a result of heterotrophic and autotrophic respiration. The description of microbial and plant CO_2 production is based on Fang and Moncrieff's model (Fang and Moncrieff, 1999). The production term S_M [M L^{-3} T^{-1}] of microbial respiration is expressed as the multiplication of an assumed maximum possible rate at which carbon decomposition occurs V_{max} [M L^{-3} T^{-1}], which depends on water content and temperature, and two different carbon pools C_{SOL} [M^{-3} L^{-3} T^{-1}] and C_{MIC} [M^{-3} L^{-3} T^{-1}]. The model accounts for a certain carbon use efficiency CUE [−], which corresponds to the fact that not all of the assimilated carbon by microbes is emitted during respiration but a fraction of it is allocated for microbial growth:

$$S_M(z,t) = V_{max}(z,t)\frac{C_{SOL}(z)}{K_m + C_{SOL}(z)}C_{MIC}(z)(1 - CUE) \tag{13}$$

where K_m $\left[\mathrm{M\ L^{-3}\ T^{-1}}\right]$ is the half-saturation constant related to the assumption that the respiration production from the C_{SOL} carbon pool follows Michaelis-Menten kinetics, with C_{SOL} the soluble soil carbon concentration. C_{MIC} is the carbon pool from organic matter produced by microbes. C_{SOL} and C_{MIC} are depth dependent carbon concentration fitted upon measured values (Ryan et al., 2018).

In their model, Samuels-Crow et al., have neglected the effect of O_2 concentration on microbial respiration to make it suitable for systems where O_2 availability is typically not a limiting factor. This adaptation is relevant for the semi-arid site that they have focused on. The CO_2 production resulting from root respiration (S_R [M L^{-2} T^{-1}]) is based on a reference root respiration rate R_{Rbase} [−], which corresponds to root respiration rate under standard soil temperature T_s [K], standard soil water content θ $\left[\mathrm{L\ L^{-1}}\right]$, the antecedent temperature T_s^{ant} [K] and antecedent water content θ_R^{ant} [L L^{-1}] values:

$$S_R(z,t) = R_{Rbase}C_R(z,t)f\left(\theta(z,t), \theta_R^{ant}(z,t)\right)g\left(T_s(z,t), T_s^{ant}(z,t)\right) \tag{14}$$

in which the mass of root carbon modeled by the C_R [M L^{-3} T^{-1}] function is calibrated on field data (Ryan et al., 2018). The f [−] and g [−] functions are used to express the dependency of autotrophic respiration on soil temperature and soil water content:

$$f\left(\theta(z,t), \theta_R^{ant}(z,t)\right) = exp\left(\alpha_1\theta(z,t) + \alpha_2\theta_R^{ant}(z,t) + \alpha_3\theta(z,t)\theta_R^{ant}(z,t)\right) \tag{15}$$

$$g\left(T_s(zt), T_s^{ant}(z,t)\right) = exp\left(E_0(zt).\left(\frac{1}{T_{ref} - T_0} - \frac{1}{T_s(zt) - T_0}\right)\right) \tag{16}$$

$$E_0(z,t) = E_0^* + \alpha_4 T_s^{ant}(z,t) \tag{17}$$

The parameters R_{Rbase} $\left[\mathrm{M\ L^{-3}\ T^{-1}}\right]$, α_1 [−], α_2 [−], α_3 [−], α_4 [−], T_0 [K], and E_0^* [K] in the model need to be assigned specific numerical values. The values of θ and T_S are direct field measurements, while θ_R^{ant} and T_S^{ant} are calculated based on field measurements. E_0^* represents the apparent temperature sensitivity of root respiration. Finally, the total CO_2 production rates for the entire soil column of a 1-meter depth, at a given time t are calculated by summing the depth specific production rates from heterotrophic and autotrophic respiration rates:

$$S(t) = \sum_{z=0.01}^{1m}\left(S_M(z,t) + S_R(z,t)\right) \tag{18}$$

CO_2 transport is modeled by Fick's law considering gas diffusion. The diffusivity coefficient is a function of atmospheric pressure, soil temperature, soil water content, and soil properties given at each depth z and time t. The description of diffusion does not consider the alterations to soil physical properties caused by plants and overlooks any potential chemical reactions occurring in the soil water. Additionally, the diffusion of dissolved CO_2 in the liquid phase is not taken into account.

To assess the performance of the model in predicting CO_2 flux R_{soil}, the results were compared with in situ CO_2 flux measurements acquired twice a month in 2008 (from April 1th to September 30th), from soil chambers placed in vegetated plots. The model output R_{soil} followed the trend observed in the field data. However, median R_{soil} measurements during the August precipitation event were up to 3 times lower than model prediction during this period. These errors are likely due to the idealized soil water content treatment in the model, different from the in situ conditions (e.g., variations in infiltration). However, despite some discrepancies, the model output fell within the 95 % credible interval of the measurements, and the coefficient of determination between measured and modeled R_{soil} indicated a high level of agreement.

The approach proposed by Ebrahimi and Or (2016) is very different from the other soil respiration models presented previously. They proposed to approach the simulation of gas fluxes from microbial communities at the millimetric scale of aggregates. They argue that it is already at this millimetric scale that the mechanisms governing the structure

and activities of microorganisms take place. For a comprehensive understanding of processes driven by trophic dependencies, it is crucial to account for cellular movement, nutrient assimilation, and growth, acknowledging how cells interact at a microscopic level within their immediate environment. Conversely, continuum or mean field models tend to overlook these intricate local interactions. The use of a model that describes trophic dependencies is justified by the fact that, even though the considered macroscopic medium is unsaturated, one can find anoxic microsites at the scale of aggregates making it possible for both aerobic and anaerobic microbial communities to coexist. In the model, the soil profile is discretized into different layers of Δz thickness, which contains aggregates of different sizes located in the bulk soil. The arrangement of aggregates within the soil profile, determined by their respective sizes, and the environmental conditions such as water, carbon, and oxygen levels vary with depth. Thus, the model can be structured into two parts, first the description of microbial activity in a single aggregate, then the upscaling technique to go from one aggregate to the whole soil profile description.

Ebrahimi and Or (2015) define the water and oxygen concentrations along with the microbial population size, composition, activity, and spatial location, at the pore scale. They simulate microbial aerobic and anaerobic activity including local interactions such as nutrient consumption, growth, division and motility, which is the microbial ability to move using their metabolic energy, with their individual-based model (Ebrahimi and Or, 2015). Ebrahimi and Or (2015) have developed a pore-scale model to quantify the spatial organization of aerobic and anaerobic microbial communities in a single soil aggregate. They assume that local GHG production rates along the aggregate radius is described by a log-normal function given by:

$$Q_{rep}(r', \mu_{aer}, \sigma_{aer}) = \frac{Q_{rep}^{max}}{\Omega_{aer}(r')} e^{\frac{(ln(r')-\mu_{aer})^2}{2\sigma_{aer}^2}} \tag{19}$$

where $r' = \frac{r}{R}$ $\left[\mathrm{L\ L^{-1}}\right]$ is the distance from the aggregate center scaled by the aggregate radius R [L]. μ and σ are the mean and standard deviation of the variable's natural logarithm, respectively. Ω is the normalization coefficient that defines gas production rate Q at the global maximum of the log-normal function. Q_{max} $\left[\mathrm{M\ L^{-3}\ T^{-1}}\right]$ is the maximum rate of gas production at the stationary state of the microbial population. The gas production depends on the carbon concentration, oxygen concentration, and water content. The reaction-diffusion Eq. (20), considering microbial consumptions, is solved to determine local carbon concentrations $[C]$, as follows:

$$\frac{\partial[C]}{\partial t]} = D_{0,[C]}\frac{\partial^2[C]}{\partial u^2} - \nu_c J_{ik} = -D_{0,[C]}A_{w,t}\frac{\partial[C]}{\partial u} \tag{20}$$

where $D_{0,[C]}$ $\left[\mathrm{L^2\ T^{-1}}\right]$ is the carbon diffusion coefficient in pure water, u is the spatial coordinate along the geometric description of a pore, ν_c $\left[\mathrm{M\ T^{-1}}\right]$ (units of mass/time or concentration/time) is the carbon consumption rate by microbial activity, and J_{ik} $\left[\mathrm{M\ L^{-2}\ T^{-1}}\right]$ is the local carbon flow rate through a connecting pore between i^{th} site to k^{th} site described by Fick's law. $A_{w,t}$ $\left[\mathrm{L^2}\right]$ is the aqueous cross section of the pore. The oxygen concentration profile within an aggregate is determined by the macroscopic conditions and the aggregate location in the soil profile. Oxygen transport in the liquid phase, necessary for aerobic microbial activity, is controlled by gas diffusion through the aggregate and dissolution rate from gas-liquid interface and then diffusion of oxygen in the liquid phase. The distributions of gas phase and water in the aggregate model are jointly determined by the matric potential in the aggregate's immediate vicinity and by geometrical characteristics of the pore network. For each aggregate size, they have considered similar pore space properties (e.g., mean pore radius sizes of 10^{-5} m and bond angularity) and similar boundary conditions for carbon and oxygen diffusions. The pore network for the simulation is constituted by 1000 to 30,000 sites for different aggregates size ranging from 1 mm to 14 mm. The total gas emitted from an individual aggregate is obtain by integrating Q_{rep} over the aggregate:

$$V_{res} = \int_{\frac{r_{an}}{R}}^{1} 4\pi Q_{rep}([C], [O_2], \theta, r')dr' \Big/ \frac{4\pi R^3}{3} \tag{21}$$

Eventually, the upscaling is operated by integrating respiration and denitrification rates from individual aggregates to estimate fluxes from an assembly of log-normally distributed aggregates of different sizes:

$$f(R) = \frac{1}{R\sigma\sqrt{2\pi}} e^{\frac{(ln(R)-\mu)^2}{2\sigma^2}} \tag{22}$$

where R is the radius of an aggregate, μ and σ are the mean and standard deviation of the aggregate size natural logarithm. Thus, the respiration rate for an assembly of aggregates $V_{ass,res}$ $\left[\mathrm{M\ L^{-3}\ T^{-1}}\right]$ is obtained by summing up the individual contributions of each aggregate class size's respiration. This calculation is based on the understanding that V_{res} $\left[\mathrm{M\ L^{-3}\ T^{-1}}\right]$ represents the respiration produced by a single aggregate:

$$V_{ass,res} = \frac{\sum R^3 V_{res}([C], [O_2]\theta, R) f(R)}{\sum R^3 f(R)} \tag{23}$$

where $[C]\left[\mathrm{M\ L^{-3}}\right]$ is the carbon concentration, $[O_2]$ $\left[\mathrm{M\ L^{-3}}\right]$is the oxygen concentration and θ is water content. The total gas production rate is obtained per unit volume of the assembly of aggregates all of which are subjected to similar macroscopic boundary conditions within a given depth element in the soil profile. The gas production rates from an assembly of aggregates may vary depending on the location in the soil profile resulting in different macroscopic boundary conditions. In their model, the soil depth is divided into different soil layers. The gas production at each layer is combined by superpositioning from the deepest layer to the surface, assuming that it is not affected by microbial activity at upper or lower depths. The resulting gas diffusion flux at depth z of the soil profile is obtained from the superposition of fluxes described by Eq. (23) that are integrated from the bottom of the soil profile:

$$J_{ass}(z') = \sum_{d_{ind}=1}^{m} (V_{ass}([C], [O_2], \theta, z)), \quad m = \frac{z'}{\Delta z} \quad \text{and} \quad z' = Z_a - z \tag{24}$$

in which d_{ind} is the layer index starting from the soil bottom, z the soil depth, and Z_a the maximum depth of the soil considered. Their formulation assumes steady-state conditions and no consumption and interaction of produced gases along the soil profile (Table 2).

As reviewed above, process-based models provide an effective method for modeling soil respiration as they combine a physical description of transport mechanisms (such as mass and heat conservation), complemented with additional terms and equations to capture complex biological processes that cannot be adequately represented by purely physical models. In this section, we have presented various process-based models, which share a consistent framework, dividing the model into two primary processes: CO_2 production and CO_2 transport (5.1). These models make simplifying assumptions to handle the highly complex nature of the ecosystem, which, when translated into a mathematical framework, becomes a set of highly nonlinear coupled mechanisms. By simplifying the models, the focus is on capturing the essential dynamics while disregarding negligible phenomena. However, the challenge lies in the dependence of such models on specific ecosystems, and achieving spatial and temporal resolution is not straightforward. It is worth mentioning that current models often assume an ideal rate of microbial respiration at positive temperatures, typically around 20 °C, which are rarely observed in permafrost conditions. Besides, carbon is not always produced as carbon dioxide but it can also be emitted back into the atmosphere as methane under specific conditions. Conse-

Table 2
Summery of soil respiration models.

Paper	Autotrophic respiration	Microbial activity	Transport Mechanisms	water flux	Heat transport	Nutrient concentration	Specificity
Šimůnek and Suarez (1993)	CO_2	CO_2	Fick's law: Gas (diffusion and convection), liquid (diffusion and convection)	Richard's equation	Conduction and heat transported by flowing water	CO_2 concentration	Root water uptake: phenomena considered as sink term in the transport of CO_2 (sink term) and in the water flux.
Fang and Moncrieff (1999)	CO_2	CO_2	Fick's law: Gas (diffusion and convection), liquid (convection)	Not described	Not described	O_2 concentration	Assume a linear relationship between root size and root respiration rate. Assume different types of carbon (labile and more resistant to decomposition).
Jassal et al. (2004)	CO_2	CO_2	Fick's law: Gas (diffusion), liquid (diffusion)	Richard's equation	Conduction and heat transported by vapor water	CO_2 concentration	Assume different types of carbon (labile and more resistant to decomposition).
Samuels-Crow et al. (2018)	CO_2	CO_2	Fick's law: Gas (diffusion and convection)	Richard's equation	Advection–dispersion equation	CO_2 concentration	Heterotrophic respiration depends on soluble carbon pool and microbial carbon pool. Autotrophic respiration defined based on a reference root respiration rate.
(Ebrahimi and Or, 2015)	Not considered	CO_2, N_2O	Radial diffusion reaction	Van Genuchten's law	Constant	C, O_2, N	Gas diffusion in aggregates.

quently, in order to effectively apply soil respiration models to permafrost regions, certain modifications are required to account for these specific conditions.

5.2. Plant-microorganisms interaction: the rhizosphere priming effect

In this review paper, we are particularly interested in the descriptions of the processes involved in CO_2 and CH_4 productions by plants and microorganisms, as well as their interaction, which is also known as Rhizosphere Priming Effect (RPE), illustrated in Fig. 4. The rhizosphere priming effect refers to the phenomenon where the presence of plant roots stimulates microbial activity and the turnover of soil organic matter in the surrounding soil, leading to an increase in the decomposition of soil organic matter. The presence of fresh organic inputs, which enhances microbial activity leads to increased decomposition rates of older more refractory organic materials, which is known as priming. The plant's inputs essentially "prime" the microbial population to break down soil organic materials faster than it would otherwise (Dijkstra et al., 2013; Jackson et al., 2019). On the one hand, it can improve plant nutrient availability by enhancing organic matter turnover and nutrient release from soil organic pools, which has the potential to boost plant productivity and thus carbon capture (*New Phytol.*, 2018). On the other hand, rhizosphere priming effect can result in increased soil carbon dioxide emissions, as it accelerates microbial decomposition of soil organic matter. Such a scenario has the potential to elevate greenhouse gas emissions, thereby making a significant contribution to climate change (Kuzyakov et al., 2018). In fact, Keuper et al. (2020) showed, by incorporating an empirical description of the rhizosphere priming effect into their model, that this mechanism could lead to a 12 % increase in soil respiration in the permafrost ecosystem (Keuper et al., 2020).

Currently, most models used to describe the rhizosphere priming effect are based on meta-analyses of empirical data, thus relying mainly on a combination of information provided by laboratory experiments and field data measurements.

Bengtson et al. (2012) have developed a model for RPE based on an experimental framework designed in-house. The model aims to understand the complex interactions between root exudation, carbon and nitrogen availability, and the decomposition of organic matter in the rhizosphere. The key components of the model include: the release of root exudates by plants into the rhizosphere, the activity of microbial communities in the rhizosphere, and the decomposition of organic matter.

The **rate of root exudation** is measured using an experimental

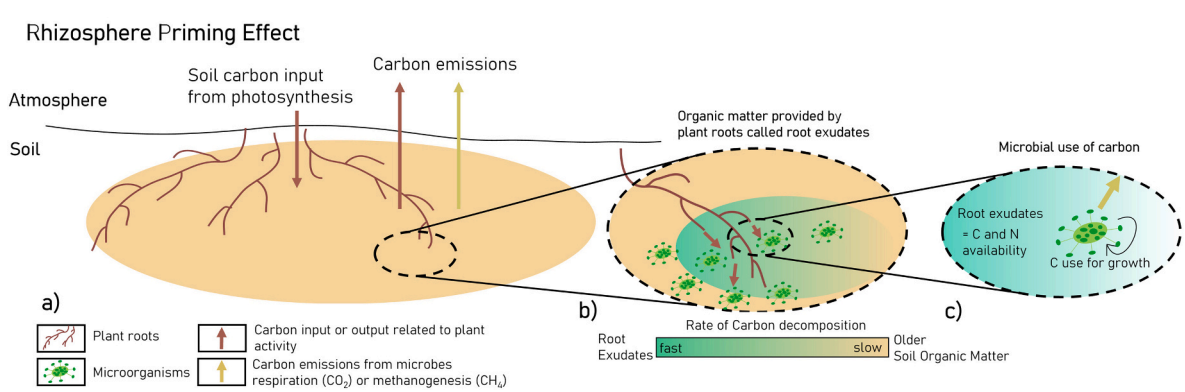

Fig. 4. Representation outlining the intricate interaction between plant roots and microbes in the carbon feedback process to the atmosphere. The Rhizosphere Priming Effect (RPE) denotes the alteration in soil organic matter (SOM) decomposition induced by root activity, leading to an increased release of nutrients that stimulate microbial activity. The figure is segmented into three sections: a) depicts the location of RPE in the vicinity of plant roots, where this local system contributes to both carbon input into the soil and carbon emissions to the atmosphere. Zooming in on the roots, b) illustrates the local input of exuded carbon provided by roots. The presence of fresh organic inputs increases microbial activity and thus the decomposition of older, more refractory organic materials. c) Microbial carbon use efficiency, which quantifies how much of the carbon decomposed by a microorganism is used for building new cellular structures, rather than being respired.

technique known as the ^{13}C pulse-chase experiment. Boxes containing grown roots are sealed and inoculated with ^{13}C-enriched CO_2. Six days after the pulse labeling, the total exudation of the ^{13}C-labeled photosynthates is determined. The rate of the supply of root exudates to the soil C_{exuded} $\left[M\ M^{-1}\ T^{-1}\right]$ is thus deduced from the measurement of $^{13}C_{soil}$ concentration:

$$C_{exuded} = {}^{13}C_{soil}\frac{t_1}{t_2}\frac{1}{\left(1 - f^{13}C_{lost}\right)} \tag{25}$$

$f^{13}C_{lost}$ $\left[M\ M^{-1}\ T^{-1}\right]$ refers to the fraction of exuded carbon that is lost, t_1 [T] indicates the length of the light period, and t_2 [T] is the duration of the labeling period.

The **activity of microbial communities in the rhizosphere** or rate of microbial carbon assimilation $C_{assimilated}$ refers to the process by which microorganisms in the soil take up and incorporate, into their biomass, carbon from organic matter. It is indeed easier to determine the microbial assimilation of native SOM from the microbial $N_{assimilated}$, which can be measured using a method involving ^{15}N, which is a stable isotope of nitrogen. Thus, $C_{assimilated}$ is calculated as the multiplication of the average $C:N_{microorganisms}$ ratio, corresponding to the proportion of carbon to nitrogen in microbial biomass, and $N_{assimilated}$ $\left[M\ M^{-1}\ T^{-1}\right]$:

$$C_{assimilated} = N_{assimilated} C:N_{microorganisms} \tag{26}$$

The decomposition of SOM $\left(SOM_{decomposed}\right)$ in response to root exudates, which represents the total carbon required by microbes for both their assimilation and respiration processes, is calculated using $C_{assimilated}$ as follows:

$$SOM_{decomposed} = \frac{C_{assimilated}}{CUE} \tag{27}$$

in which CUE [−] is the microbial carbon use efficiency, which quantifies how much of the carbon acquired by an organism is retained and used for building new cellular structures, such as tissues and biomass, rather than being respired. A high CUE indicates that a significant portion of the acquired carbon is converted into new biomass, reflecting efficient carbon utilization and high growth potential. Conversely, a low CUE suggests that a larger proportion of the acquired carbon is lost through respiration or other metabolic processes (Adingo et al., 2021; Geyer et al., 2016).

Finally, the researchers have compared the total SOM decomposition $\left(SOM_{decomposed}\right)$ with the amount of SOM decomposition in the absence of root exudates. The difference of these two quantities enables them to define the SOM decomposition related to priming, in other words, related to the release of root exudates. Their experiments have shown that the priming effect resulted in an increase in SOM decomposition of between 56 % and 244 % depending on the vegetation species considered in the experiment (Bengtson et al., 2012).

Chertov et al. (2022) have developed a model to account for the process of the plant-soil interaction. The model considers how increased SOM mineralization, influenced by the $C:N$ ratio of both soil and root exudates, compensates for nitrogen deficiency required for microbial growth. Moreover, the model introduces a food web procedure that computes interactions between soil fauna and microorganisms, corresponding to faunal by-products returning to SOM and the production of mineral nitrogen that can be taken up by plant roots.

Root exudates are known to contain nitrogen compounds, which serve as crucial resources for the growth of soil microorganisms. Nonetheless, it is acknowledged that the exudates may sometimes lack sufficient nitrogen content to efficiently support microbial growth. The model's structure comprises three subroutines:

- Modeling of microbial growth related to the available carbon and nitrogen derived from root exudates and the related microbial respiration.
- Modeling of microbial growth related to the utilization of residual carbon from root exudates and the nitrogen extracted from the soil organic matter in the rhizosphere, which is what they call "N mining", and the corresponding microbial respiration.
- Modeling of the formation of faunal by-products, which corresponds to the creation of nitrogen compounds through the feeding of soil fauna on microorganisms.

The modeling of microbial growth related to root exudates is based on the description of changes in microbial biomass carbon, C_{MO} $\left[M\ L^{-2}\right]$, due to root exudate consumption over time, which they formulate as follows:

$$C_{MO}(t + \Delta t) = C_{MO}(t)\left(1 - K_f\right) + \Delta C_{MO} K_{AS} \tag{28}$$

where K_f $\left[T^{-1}\right]$ is the rate at which soil fauna feed on microorganisms, K_{AS} $\left[T^{-1}\right]$ is the rate at which microorganisms assimilates root exudates, ΔC_{MO} $\left[M\ L^{-2}\right]$ is the daily increment of microbial biomass, which is estimated as the multiplication of the microbial community's $C:N$ ratio, and ΔN_{RE} $\left[M\ L^{-2}\right]$ is the nitrogen daily flow in root exudates.

Besides, a part of the root exudates consumed by microbes is used for respiration and this respiration daily flow is given by:

$$\Delta R_{MO} = \Delta C_{MO}\frac{\left(1 - K_{eff}\right)}{K_{eff}} \tag{29}$$

where K_{eff} [−] is the carbon-assimilated exudates growth efficiency factor for microorganisms.

Within the second subroutine, the microbial growth related to the use of excessive carbon of exudates and mined nitrogen from the rhizosphere soil organic matter are evaluated. They assumed that a residual part of the carbon remains in exudates as it cannot be utilized for microbial growth when all nitrogen in exudates has already been used. However, nitrogen is recovered, which they called *nitrogen mining*, by the mineralization of rhizosphere soil organic matter. Eventually, an additional daily flux of microbial respiration related to the consumption of the residual carbon ΔR^{+}_{MO} is given by:

$$\Delta t R^{+}_{MO} = \Delta C^{rest}_{RE}\left(1 - K_{eff}\right) \tag{30}$$

in which ΔC^{rest}_{RE} $\left[M\ L^{-2}\right]$ is the daily increment in residual carbon. Another flux of microbial respiration is taken into account, which is related to the process of nitrogen mining necessary to the use of excessive carbon C^{rest}_{RE} $\left[M\ L^{-2}\right]$. This flux of CO_2 emission related to microbial respiration during N mining corresponds to what is called the real priming effect given by:

$$R_{NM} = N_{NM} CN_{SOM} \tag{31}$$

where N_{NM} $\left[M\ L^{-2}\right]$ is the amount of nitrogen that needs to be mined, and CN_{SOM} $\left[M\ L^{-2}\right]$ is the rhizosphere soil $C:N$ ratio.

In the third subroutine of the model, Chertov et al. (2022) account for the carbon production related to the consumption of microorganisms by microbial grazers (protozoans, nematodes, and microarthropods), and the related respiration. The respiration of microbial grazers, ΔR_{MG}, is calculated as follows:

$$\Delta R_{MG} = \Delta C_{fa}\left(1 - K_{MG}\right) \tag{32}$$

where ΔC_{fa} $\left[M\ L^{-2}\right]$ is the total carbon of microorganisms assimilated by soil fauna, and K_{MG} [−] is the coefficient of assimilation of food by microbial grazers (production efficiency).

The cumulative rhizosphere priming effect is determined by summing up the three components calculated in each of the three subroutines. The total daily CO_2 emission related to root exudates input into the rhizosphere is given by:

$$\Delta R_{tot} = \Delta R_{MO} + \Delta R_{MO}^{+} + \Delta R_{MN} + \Delta R_{MG} \tag{33}$$

where $\Delta R_{MO} + \Delta R_{MO}^{+}$ $\left[\mathrm{M\ L^{-2}\ T^{-1}}\right]$ represents microbial respiration due to root exudation consumption, ΔR_{MN} relates to soil organic matter mineralization at nitrogen mining, and ΔR_{MG} corresponds to the respiration of food web. The simulation results provide a quantitative evaluation of the priming effect's contribution to the overall CO_2 emission, estimating that this process can account for 30 to 40 % of the total CO_2 emission from the entire soil.

Keuper et al. (2020) proposed a model to better understand the influence of climate change on carbon release from permafrost soils in the northern circumpolar areas, with a particular emphasis on the function of the rhizosphere in accelerating carbon loss. This large-scale model consists of three modules: **Soil module**, **Plant module** and **Soil Respiration module**.

The **soil module** focuses on estimating the quantity of soil organic carbon (SOC) stored in the northern permafrost region. They obtain the amount of SOC in soil from the Northern Circumpolar Soil Carbon Database. This module also assumes that microbial carbon limitation can be an effective factor in estimating RPE. Microbial carbon limitation occurs when the $C:N$ ratio of the soil organic matter falls below a specific amount.

In the **plant module**, since the RPE is driven by the transfer of organic compounds from plants to the soil, the activity of plant roots seems to be an important factor to be considered. Therefore, for evaluating this connection, they derive the RPE ratio function, representing the relationship between the CO_2 released from the soil because of RPE and the carbon absorbed by plants via photosynthesis. This correlation between root respiration and RPE ratio has been established through a meta-analysis of previous studies, which led to the following empirical relationship:

$$RPE_{\mathrm{ratio}} = 1 + \frac{2.47(\text{root respiration})}{13.01 + (\text{root respiration})} \tag{34}$$

where *root respiration* is obtained from Gross Primary Production (GPP), which represents the amount of energy that plants create through photosynthesis in a given length of time. Previous studies provided current annual GPP estimates for the northern permafrost area (Beer et al., n.d.). The projected GPP in the year 2100 is estimated for two different representative concentration pathways, RCP 4.5 and RCP 8.5, which are used to represent different greenhouse gas emission scenarios and their potential impacts on global climate change. RCP 4.5 represents a scenario where global greenhouse gas emissions peak around the year 2040 and then gradually decline. It is considered a medium-to-low emissions scenario and assumes significant efforts to reduce greenhouse gas emissions. RCP 8.5, on the other hand, represents a high emissions scenario with no specific climate mitigation policies or efforts to curb greenhouse gas emissions.

In the **soil respiration module**, soil respiration is calculated based on two different scenarios: baseline soil respiration in which RPE is not considered and RPE-affected soil respiration. They estimate basal respiration rate based on *GPP* values, which is the production of CO_2 under the current climate situation. *GPP* can serve as an indicator of favorable climate conditions that support both plant growth and carbon release. Higher *GPP* values generally indicate more favorable environmental conditions for plant growth, such as higher temperatures, sufficient water availability, and adequate sunlight. The basal soil respiration has been estimated as an exponential function of *GPP*:

$$\frac{Rh}{SOC} = A^{*} GPP^{B} \tag{35}$$

where $\frac{Rh}{SOC}$ is the heterotrophic respiration, A and B are model constants calculated based on experimental data. For the second scenario, which is calculating the carbon release related to plant-microbe interaction, they used the RPE_{ratio}, which shows the influence of plants, and the basal soil carbon respiration rates calculated in the first scenario. For specific areas where the soil is seasonally thawed, plants are actively growing ($GPP > 0$), and the microbial carbon limitation becomes relevant below a $C:N$ threshold of 20. They calculated the carbon release affected by both plants and microbes by multiplying the basal soil carbon respiration estimate $\frac{Rh}{SOC}$ with the RPE_{ratio}. Finally, they assessed soil respiration in permafrost with and without RPE under current and future climatic conditions. According to their findings, the RPE would result in an increase in carbon release from permafrost by 0.40 petagrams (Pg) of carbon per year under the current climate change scenario. In 2100, the predicted extra soil respiration due to RPE would be 0.43 Pg/yr for RCP 4.5 and 0.49 Pg/yr for RCP 8.5. They predict that between 2010 and 2100, the RPE might result in a cumulative loss of 38 Pg SOC to the atmosphere for RCP 4.5, and 40 Pg SOC for RCP 8.5. This suggests the importance of RPE in determining the carbon budget of permafrost.

RPE models provide detailed descriptions of microorganism-scale processes, which were not explicitly considered in the large-scale carbon feedback models discussed in subsection 5.1. The earlier-presented land surface models merely accounted for carbon feedback contributions from plants and microorganisms, without describing the underlying processes and interactions between roots and microbes. Consequently, the explicit consideration of the interaction between plants and microbes was absent from the models, with their combined contributions treated as a whole. However, research on RPE has demonstrated that neglecting the mechanisms linking the behavior of plants and microbes leads to an underestimation of carbon emissions. Recently, several papers have been published to describe microbial activity, growth, and respiration, which are influenced not only by carbon availability but also by the quantity of nitrogen (Aqeel et al., 2023; Singh et al., 2023; Stark et al., 2023). These studies have highlighted that microbial activity is stimulated by the nutrients supplied by plant roots, a phenomenon that was not previously well-documented or described. Fig. 4 illustrates this relationship.

Nevertheless, the reliance of the current model on experimental data obtained from specific microcosms may limit its ability to encapsulate any ecosystems. As an example, Bengtson et al. (2012) conducted experiments that showcased how RPE led to varying increases in SOM decomposition across different vegetation types. Their findings revealed a 154 % increase in SOM decomposition for western hemlock and a more substantial 244 % increase for sitka spruce (Bengtson et al., 2012). In addition to different vegetation types and microorganism species, the effects of seasonal changes in permafrost ecosystems must also be considered. The freezing and thawing of the active layer, and the potential for a suprapermafrost talik, has an impact on the quantity of nutrients available, and therefore on the activity of plants and microbes. The seasonal changes also bring attention to the time frame considered in the model. In some instances, the model assumes rapid consumption of all nitrogen in exudates and a fraction of carbon by microbes within fixed time steps. These simplifications may oversimplify microbial nutrient uptake kinetics, which could introduce potential inaccuracies in predictions, especially when nutrient availability fluctuates, or other factors influence microbial growth responses.

6. Mathematical models for PCF

Permafrost ecosystems, in particular, pose a significant challenge for process-based modeling due to their diverse range of temperatures, moisture content, unfrozen water content, vegetation types, and microbial communities. The complexity stems from the presence of distinct conditions within permafrost, including a permanently frozen layer and a seasonally thawing active layer. Moreover, the presence of thermokarsts and taliks, which are thawed regions penetrating the permafrost and potentially forming subterranean lakes, contributes to distinct ecosystem characteristics at a local level. Additionally, permafrost ecosystems exhibit a wide range of vegetation types, from mosses and

lichens to shrubs and trees, which impact nutrient distribution, carbon inputs, and root-associated microbial communities. Vegetation also plays a role in soil insulation, influencing both soil temperature and soil moisture. As a result, permafrost is home to diverse microbial communities with varying metabolic capacities, which can interact in complex ways. For that, developing a comprehensive process-based model that accurately captures the dynamics of GHG emissions in permafrost ecosystems is a substantial challenge.

When it comes to modeling carbon production and carbon transport from permafrost ecosystems, as represented schematically in Fig. 5, many interacting mechanisms and parameters need to be taken into account. We have already discussed in the previous section, the CO_2 production from plants and microorganisms by what is called soil respiration. But the production of CH_4 also needs to be addressed as it is responsible for up to one-third of near-term global warming, according to the Intergovernmental Panel on Climate Change (IPCC) (Core Writing Team et al., 2023). Moreover, the permafrost ecosystem is particularly favorable to methane production, with the presence of talik creating anaerobic conditions and the presence of methanogens among endogenous microorganisms. The mechanisms of carbon transport are also modified in permafrost regions as compared with the mechanisms described previously for soil respiration due to the fact that water is present in both liquid and solid phases. The phase change has consequences on the water flux and thus on the soil moisture along the soil profile. Permafrost is a complex and evolving ecosystem, and mathematical models for predicting carbon feedback in these regions are continually being refined and updated to improve our understanding of the underlying mechanisms. Numerical modeling can prove to be an effective approach for researching permafrost microbiology and its influence on greenhouse gas emissions. In practice, numerical models provide a means to test hypotheses and simulate the large-scale and long-term carbon feedback from a challenging-to-access region of the world. Furthermore, these models allow for the exploration of various climate change scenarios. The ability to simulate different climatic conditions becomes particularly valuable since scientists are still struggling to predict the extreme climatic events likely to occur in the coming years. Nevertheless, constructing a sufficiently robust numerical model is a complex process that requires significant effort to identify and integrate the key mechanisms responsible for greenhouse gas emissions.

Wania et al. (2010) developed the LPJ (Lund-Potsdam Jena Dynamic Global Vegetation Model) model, which is a large-scale process-based model, that they modified to make it able to model methane emissions from northern peatlands. They implemented a dynamic global vegetation model to estimate methane emission from the active layer. LPJ includes plant physiology, carbon allocation, methane production, oxidation and transport, and hydrological fluxes.

Plant physiology: The LPJ model categorizes vegetation into groups called Plant Functional Types (PFTs) based on similar characteristics. It models the survival and growth of these PFTs by accounting for their required temperature for growth, as well as the minimum and maximum temperatures they can endure. Climate conditions, such as precipitation, are also considered to define soil moisture, influencing methane and carbon dioxide production and transport. To adapt LPJ for peatland regions, Wania et al., introduced two new plant types: flood-tolerant C_3 graminoids and Sphagnum mosses, which are typical plant types found in wetland areas.

Carbon allocation: The carbon pool available consists mainly of root exudates, easily degradable plant material, and in a smaller portion of more recalcitrant organic matter. The carbon pools are distributed across the soil layers and weighted by root distribution. More carbon is allocated to the upper layers where root density is greater than in the bottom layers. At that point, the model can be divided into two main components. First, methane and carbon dioxide production then their transport through the soil layers. The transport of O_2 is also modeled to account for the oxidation of a fraction of the methane into carbon dioxide. A schematic of the processes represented in the model are presented in Fig. 6. In their model, they assumed that both methane and carbon dioxide are produced through microbial decomposition of carbon originating from different carbon pools. The potential carbon pool forms through the breakdown of litter into slow and fast soil carbon pools, along with exudates. Each of these soil carbon pools is characterized by decomposition rates dependent on temperature and moisture. These rates govern their conversion into the potential carbon pool for methanogens. From the potential carbon pool, methane and carbon dioxide are produced, with the methane-to-carbon dioxide ratio varying between 0.001 and 1.7. This ratio hinges on the level of anoxia within

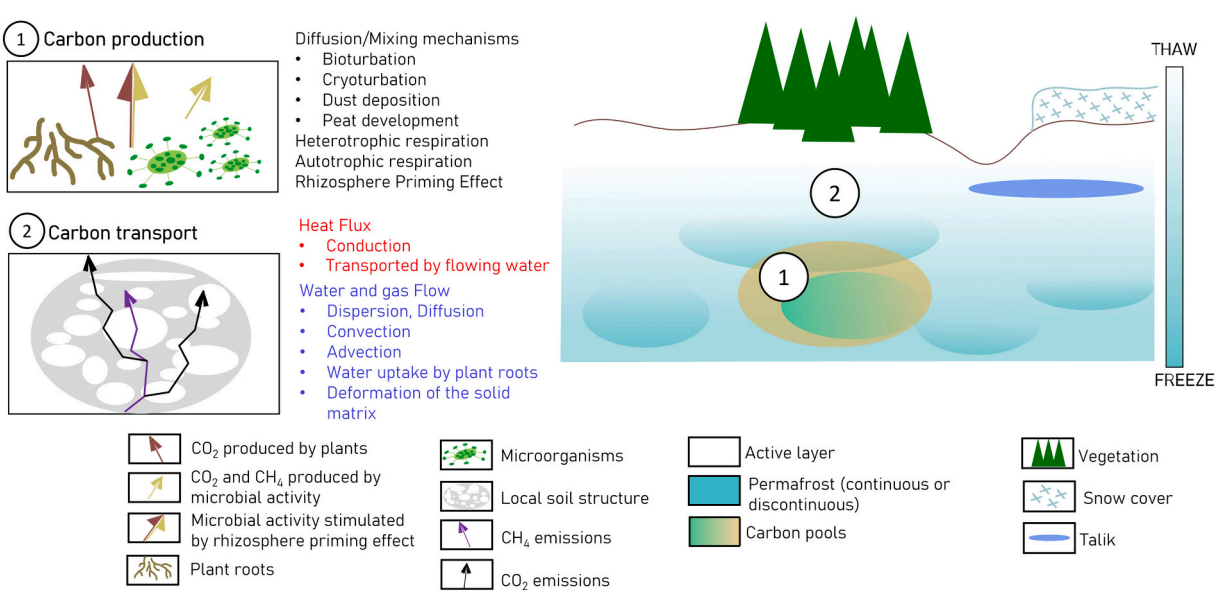

Fig. 5. Emissions of greenhouse gases from permafrost occur in two stages: initially, the production of CO_2 and/or CH_4, followed by their transport through the soil towards the atmosphere. Both production and transport are highly affected by local permafrost conditions (vegetation type, microorganisms types, soil moisture, soil temperature, soil porosity and tortuosity). 1) The production of carbon depend on the quality of the organic matter, the presence of nutrients such as nitrogen and the interaction between the different types of vegetation and the microorganisms. 2) Different transport mechanisms explained the emissions of CO_2 and/or CH_4 to the atmosphere.

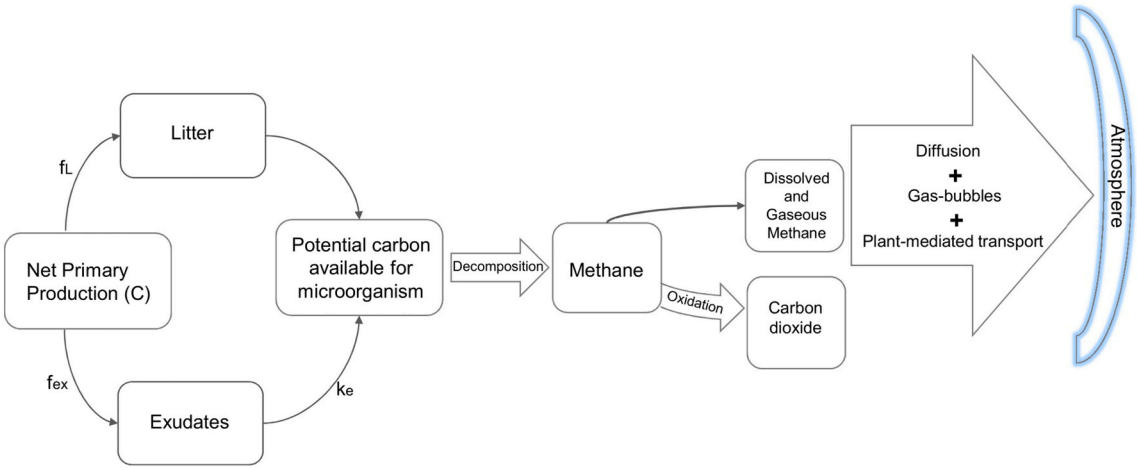

Fig. 6. Scheme representing LPJ model developed by Wania et al. (2010). This figure shows the different processes involved in this model. *k* stands for a constant rate to account for the decomposition of more or less easy to decompose carbon and *f* represents the proportion of the carbon pool that goes directly to another pool.

the particular soil layer under consideration. The parameters are initially calibrated for condition of full inundation and subsequently refined considering the level of anoxia, determined by the air content in the layer. This adjustment influences the decomposition process accordingly.

The second part of the model deals with the transport of methane, carbon dioxide and oxygen across different soil layers. Specifically, the model accounts for the transport of oxygen, to account for the fact that a portion of the produced methane is converted into carbon dioxide during transport, thereby reducing the overall methane emissions. Methane transport is assumed to happen through three different pathways: diffusion, plant-mediated transport, and gas-bubble ebullition. On the other hand, oxygen and carbon dioxide are assumed to be only transported either by diffusion or plant-mediated transport.

The transport of CH_4, CO_2, and O_2 through diffusion obeys Fick's law, except when approaching the water-air interface. To accurately calculate the gas flux *J* from the upper layer into the overlying air layer, an adjusted method is employed given in Eq. (36). This adaptation accounts for the substantial four-order-of-magnitude rise in gas diffusivity at this boundary, ensuring a more precise estimation of the gas movement.

$$J = -\Psi\left(C_{\text{surf}} - C_{\text{eq}}\right) \tag{36}$$

in which Ψ is the gas exchange coefficient with units of velocity, C_{surf} is the concentration of gas measured in the surface water, and C_{eq} is the equilibrium concentration of gas in the atmosphere. To accommodate diffusion in both liquid and gaseous fluids, the diffusivity coefficient is modified to reflect diffusion in either the gaseous or liquid phase. This adjustment relies on the percentage of air contained within that specific soil layer. When the air fraction f_{air} is less than or equal to 0.05, the dominant mechanism is considered to be diffusion in the water pore. However, when f_{air} is higher than 0.05, gas diffusion is assumed to be the dominant mechanism. The diffusivity coefficients both for gaseous diffusion and diffusion in water are adapted to vary with soil temperature. Moreover, they also account for the effect of soil porosity on gas diffusivity, by multiplying the gas diffusivity coefficients by $f_{air}^{\frac{10}{3}}/\Phi^2$, with Φ the soil porosity.

Another transport pathway for methane from the soil to the atmosphere, along with the transport of oxygen entering the soil, occurs through gas-filled tissues found in roots, rhizomes, stems, and leaves, known as *transport through aerenchyma*. The gas movement through plant tissues is generally either passive, following concentration gradients, or actively pumped upwards. This model only considers the passive aerenchyma transport. Key parameters selected to describe the transport mechanisms are as follows:

- The presence and abundance of specific plant species capable of aerenchyma transport.
- The quantity of methane being transported within these plants, as a significant proportion of methane is oxidized in the highly oxic zone around the roots. The extent of methane oxidation, ranging from 20 % to 100 %, depends on the vegetation type (Ström et al., n.d.).
- The availability of plant cells for gas transport.
- The allocation of plant cells to facilitate gas transport in correspondence with the quantity of plant roots present in each soil layer.

The third transport mechanism considered in this model for methane transport is *gas-bubble ebullition*. It occurs when the concentration of dissolved gases in the water exceeds the equilibrium concentration, which corresponds to the methane maximum solubility. When the gaseous molecules of methane cannot dissolve in water anymore the pressure build up leading to the formation and subsequent release of gas bubbles. The solubility coefficient S_B is fitted Yamamoto et al.'s observations (Yamamoto et al., n.d.):

$$S_B = 0.05708 - 0.001545T + 0.00002069T^2 \tag{37}$$

in which S_B represents the volume of gas dissolved per volume of liquid at the atmospheric pressure and at a given temperature *T*.

The overall CH_4 flux from the soil to the atmosphere is represented by the sum of ebullition, diffusion, and plant-mediated transport. The parameters of the model are calibrated using monthly measurements of the different methane fluxes, i.e. plant-mediated, diffusion, ebullition, and total flux, in seven different sites, except for seven parameters ($\frac{CH_4}{CO_2}$ production ratio under anaerobic conditions, Fraction of available oxygen used for methane oxidation, Fraction of Net Primary Production put into exudates pool, Turnover rate for exudates pool, Moisture response used to weight decomposition rates for carbon pools, Tiller porosity and Tiller radius) for which the lack of available data forced them to estimate their values by conducting sensitivity tests. The in situ observations were conducted between 1989 and 2006. They identified a unified set of model parameters applicable across all sites, selecting the parameter set that minimizes the overall error, as measured by RMSE (root mean square error). Yet, they also demonstrate the enhanced performance potential of the model through site-specific calibration. With the optimal overall parameter set, they were able to estimate the contributions of each flux type to the total flux across the seven sites. The plant-mediated transport represents between 69.9 % and 84.5 %, the diffusion between 15.5 % and 30.9 % and the gas-bubble ebullition

between 0 % and 1.4 %. Naturally, calibrating parameters for a specific local area and subsequently using them to model a larger area introduces some error. The comparison of the model to measured values for specific sites enables the authors to address these errors. Further, the spatial and temporal resolution of the model parameters may be at stake. The authors could associate lower predicted methane emission values from their model than measured field data and incorrect timing of emissions with local topographic heterogeneity that were not taken into account in the model parameters, which results from the overall best parameter set. In the same way using monthly data rather than daily data may prevent the model from predicting peak emissions.

Schneider von Deimling et al. (2015) have developed a large-scale two-dimensional multi-pool model to predict the release of carbon dioxide and methane from thawed permafrost in Yedoma regions. Yedoma is a type of permafrost landscape found in the Arctic and subarctic regions. It is characterized by extensive deposits of organic-rich soil. This model is based on the model for the assessment of greenhouse gas induced by climate change (MAGICC) developed by Meinshausen et al. (2011). MAGICC is a compartmental model, which simplifies the exchange of carbon dioxide between distinct components of the Earth's terrestrial ecosystems by employing a series of compartments to represent different carbon pools. The definition of the different compartments is based on the assumption that carbon permafrost feedback stems from both near surface carbon pool, which corresponds to the active layer, and from deeper carbon pool, which corresponds to frozen soil. The objective is to comprehend the division of vulnerable carbon stored in permafrost into pools that are near the surface and those that extend deeper within the permafrost layers. The carbon is subdivided into different sub-pools based on soil-physical parameters, hydrologic circumstances, and organic matter quality. The distribution of soil carbon content in each pool has been estimated based on data from the Northern Circumpolar Soil Carbon Database which is a geographical dataset of the organic carbon storage in soils in the northern circumpolar permafrost zone.

To estimate CO_2 and CH_4 production from each carbon pool, the researchers make assumptions about fast and slow carbon decomposition within these pools. In the fast carbon pools, CH_4 production primarily results from acetate fermentation of labile organic matter. They apply a 1:1 production ratio of CH_4:CO_2 for anaerobic conditions, following the stoichiometry of CH_4 production through this pathway. However, for the slow carbon pools, CH_4 production follows alternative pathways with different electron acceptors. This leads to reduced CH_4:CO_2 production ratios for anaerobic conditions, which is assumed to be 1:7. The transport mechanism for CO_2 and CH_4 depends on the depth of the carbon pool. For the release of CH_4 from thermokarst pools, ebullition is the primary pathway, while other modes of transport are negligible. For CH_4 release from wetlands pools, methane emitted from pools travels through numerous pathways, with oxidation being an important process that influences its eventual release into the atmosphere.

PCF is released to atmosphere, as CO_2 and CH_4, from each different soil carbon pool C, under aerobic or anaerobic conditions, from different organic matter qualities, at specific latitudes, and depth levels is described as follows:

$$C(t) = R(t)VC(t) \tag{38}$$

where R is the carbon release rate and VC is the pool-specific amount of carbon vulnerable to decomposition. The model comprises a total of 24 carbon pools, which can be categorized into four main types: organic and mineral pools for both surface and deep carbon, resulting in a total of four distinct pools. Besides the production of methane and carbon dioxide is either under anaerobic and aerobic conditions for each pools, which means that eight different C coefficients are defined. These parameters have specific amounts for each soil carbon pool.

The model is calibrated with field data and predicts CO_2 and CH_4 emission from Yedoma regions of Siberia and Alaska under different climate change scenarios. While forecasting PCF under medium and high greenhouse gas emission scenarios, the researchers discovered that short-term studies suggested a relatively small permafrost feedback, which appeared unreasonable. They found that the climatic impacts of thawing permafrost became more apparent after the 21st century. Additionally, when projecting methane transport under the worst-case scenario, the model presented lower values compared to measured field data, particularly in wetland-affected sediments. This discrepancy may be attributed to the fact that the model calculates greenhouse gas emissions from newly thawed permafrost but neglects to consider carbon fluxes from the current active layer. Another potential reason for this mismatch is the oversight of abrupt thawing under thermokarst lakes, which could lead to peak CH_4 emissions.

There are only a few mathematical models that thoroughly account for the complexities of microbial activity within permafrost when simulating carbon feedback. Comprehending the metabolic rates and behaviors of microbes within soil aggregates on a smaller scale could hold considerable importance in the broader model of PCF. Ebrahimi et al. explored this aspect in their work (Ebrahimi, 2017). The biophysical model designed to quantify methane production, consumption, and transport is first created for individual soil layers. Subsequently, it's scaled up to simulate methane dynamics across the entire soil profile. The transport processes of methane across the soil layers are assumed to be diffusion and ebullition, while vegetation as transport mechanism has been neglected. The model is coupled with permafrost freezing and thawing, along with hydrological processes that consider variations in water table levels and liquid saturation along the soil depth. This coupling provides depth-dependent macroscopic boundary conditions for oxygen, water, and temperature across the soil profile.

In their study, Ebrahimi (2017) simulated the **methane production** by modeling the physiological mechanisms of methanogens and methanotrophs cells. They employed an Individual-Based Model, which they previously developed in another paper (Ebrahimi and Or, 2014), to simulate microbial communities within simplified soil pore spaces. This involves accounting for processes such as their dispersal, growth, division, as well as nutrient and oxygen consumption. They also account for enzymatic activity, which is the producing of enzymes by microorganisms that facilitate the breakdown of complex soil organic matter. Through enzymatic action, organic matter is transformed into simpler compounds like dissolved organic carbon and nitrogen. The production rate of dissolved carbon $D_{[C]}$ is determined by the amount of enzyme carbon present in each tiny space of the pore network as follows:

$$D_{[C]} = K_D \frac{E_{[C]}}{K_{s,enz} + E_{[C]}} \tag{39}$$

where the constant K_D $\left[\mathrm{M\ L^{-3}}\right]$ represents the rate of decomposition for particulate soil organic carbon. The half-saturation constant, $K_{s,enz}$ $\left[\mathrm{M\ L^{-3}}\right]$, indicates the concentration at which the enzymatic activity becomes half of its maximum. The overall enzyme carbon, $E_{[C]}$ $\left[\mathrm{M\ L^{-3}}\right]$, accounts for the total enzyme concentration, including enzymes present both within and outside the cells. The process of decomposing soil organic carbon is linked to the decomposition of soil organic nitrogen through the soil $C:N$ ratio, which is assumed to be evenly distributed across the soil profile.

The simulation starts by uniformly introducing 1000 methanotrophs and 1000 methanogen cells into each pore of the networks. Following cell inoculation, they disperse throughout the entire network and undergo various processes, including enzyme production, nutrient consumption (carbon for methanogens and methane/oxygen for methanotrophs), growth, and division into new daughter cells. The growth dynamics of both methanogens and methanotrophs is modeled by two Monod-kinetic Eqs. (40) and (41). The rate at which dissolved organic carbon is uptaken by methanogens $\nu_{[C]}$ is as follows:

$$\nu_{[C]} = s\frac{V_{max}^{Mgen}[C]}{K_{[C]}+[C]}\frac{K_{inh}}{[O_2]+K_{inh}} \tag{40}$$

and the rate at which methane is uptaken by methanotrophs $\nu_{[CH_4]}$:

$$\nu_{[CH_4]} = s\frac{V_{max}^{Mtroph}[CH_4]}{K_{[CH_4]}+[CH_4]}\frac{[O_2]}{[O_2]+K_{[O_2]}} \tag{41}$$

in which [C], $[CH_4]$, and $[O_2]$ refer to the concentrations of carbon, methane, and oxygen, respectively. s[M] is the cell dry mass of the individual bacteria calculated by multiplying the cell density by the cell volume. The model incorporates the influence of carbon and oxygen by considering their respective half-saturation constants, denoted as $K_{[C]}$ and $K_{[O_2]}$. Additionally, an oxygen inhibition constant, K_{inh}, is included in the anaerobic growth kinetics to account for the oxygen-sensitive growth of anaerobic species. The maximum specific growth rate V_{max}^{Mgen} $\left[T^{-1}\right]$ and V_{max}^{Mtroph} $\left[T^{-1}\right]$ denotes the highest rate at which methanotrophs and methanogens can consume specific nutrients. For permafrost conditions, the maximum specific growth rate for either methanotrophs or methanogens is modeled as a function of the surrounding temperature:

$$V_{\max} = \frac{(b_3(T-T_{\min}))^2(1-exp(c_3(T-T_{\max})))}{Y_{\max}} \tag{42}$$

where b_3 and c_3 are empirically fitted parameters, $Y_{\max}$ $\left[T^{-1}\right]$ represents the growth rate of microbes, and $T_{\min}$ and $T_{\max}$ are minimum and maximum temperature of the surrounding area.

The principal **methane transport** pathways in their study are gas diffusion through unsaturated soil and gas bubble ebullition, while transport through the plant tissues is not described here. The methane production and consumption in each soil layer are upscaled to simulate them over the soil profile. Each layer within the soil profile contains a volume fraction of soil aggregates f_{agg} and a bulk soil fraction f_{bulk}. The total gas production or consumption rates at each layer are obtained by integrating the production/consumption rates (S_{agg}) over aggregates of different sizes and considering the fraction of bulk soil (S_{bulk}) to give the gas production/consumption rate from a specific layer. The total methane diffusive flux from aggregates and bulk soil for a given layer $S_{\text{d,diff}}$ is given as:

$$S_{\text{d,diff}} = f_{\text{agg}}\left(\frac{\int_R^3 S_{\text{agg}}f(R)\,dR}{\int_R^3 f(R)\,dR}\right) + f_{\text{bulk}}S_{\text{bulk}} \tag{43}$$

where R is the aggregate size and $f(R)$ is the assumed lognormal distribution of aggregates in a soil layer. The process of gas bubble ebullition occurs when the concentration of dissolved gases in the water exceeds the equilibrium concentration, which corresponds to the methane solubility. This condition is frequently associated with poor dissolved methane diffusion. As a result, bubbles of methane nucleates in soil pores and aggregates every time that the concentration of methane goes above a specific threshold value. The methane solubility is assumed to be exponentially related to temperature:

$$Sol_{\text{CH}_4} = 38.76exp(-0.021\text{T}) \tag{44}$$

As a first approximation, gas bubble ebullition is modeled by considering a threshold value for bubble sizes, which introduces stochasticity in the relationship between methane gas storage and release dynamics. When methane storage in a model domain exceeds the release threshold, the entire stored methane gas is instantaneously released, travels to the soil surface, and is emitted to the atmosphere. Ultimately, the total methane flux at the soil surface comprises two components: a relatively steady diffusive flux and sudden bursts of methane bubbles released through ebullition.

The model is coupled with heat and mass transfer to account for the thawing process. The changes of soil temperature and the thickness of the active layer are assumed to be coupled. So, they divide the temperature changes into two separate transient heat conduction equations based on the thickness of the active layer as follows:

$$\alpha\frac{\partial^2 T}{\partial z^2} = \frac{\partial T}{\partial t} \quad for \quad 0 <= z <= Z \tag{45}$$

Frozen zone:

$$\alpha_f\frac{\partial^2 T'}{\partial z^2} = \frac{\partial T'}{\partial t} \quad for \quad Z < z < \infty \tag{46}$$

in which T and T' represent the temperature distribution in the thawed and frozen zones, respectively. The variables α $\left[L^2\ T\right]$ and α_f $\left[L^2\ T\right]$ correspond to the bulk thermal diffusivity of the thawed and frozen zones, respectively. Additionally, Z denotes the position of the thawing front within the soil.

At the boundary between the frozen and thawed zones, the energy balance is established by equaling the conductive heat flux from the thawed zone to the energy needed for thawing, considering the enthalpy of fusion, and the conductive heat flux to the frozen zone as follows:

$$-\lambda\frac{\partial T(Z,t)}{\partial z} = S_{wf}\rho_w\epsilon L_f\frac{dZ}{dt} - \lambda_f\frac{\partial T'(Z,t)}{\partial z} \tag{47}$$

in which S_{wf} represents the liquid water saturation in the thawed zone, ρ_w $\left[M\ L^{-3}\right]$ is the density of liquid water, ϵ is the soil porosity, L_f $\left[M\ L^2\ T^{-2}\ M^{-1}\right]$ is the enthalpy of fusion for water, and λ $\left[M\ L^2\ T^{-3}\ C\right]$ and λ_f $\left[M\ L^2\ T^{-3}\ C\right]$ represent the bulk thermal conductivity of the thawed and frozen zones, respectively.

During the arctic fall season, the refreezing phenomenon in unsaturated soil was depicted using a simplified solution of energy and mass conservation. The water state within the soil profile is characterized by a one-dimensional mass conservation model, as follows:

$$\frac{\partial(M_w+M_i)}{\partial t} + \nabla(J_w) + S_w = 0 \tag{48}$$

where M_w and M_i represent the mass of water and ice, respectively, within the soil volume. S_w is a sink term denoting water loss due to processes like evaporation or root water uptake, while J_w $\left[L\ T^{-1}\right]$ represents the water flux obtained from the Richards equation. For simplicity, the assumption is made that both S_w and J_w are equal to zero, meaning that no drainage is considered in the model.

The energy conservation within the soil volume is expressed as follows:

$$\frac{\partial U}{\partial t} + \frac{\partial(q_c+J_{adv})}{\partial z} + S_{loss} = 0 \tag{49}$$

where U represents the total internal energy of the solid particles, ice, and liquid phases, q_c represents the conductive heat flux, J_{adv} is the convective heat flux, and S_{loss} represents the sink term accounting for energy losses to the soil depth.

For an unfrozen profile, the two main unknowns are the water content and temperature profiles, which are directly obtained from the mass and energy conversion equations (). For two growing seasons, they forecast the seasonal change of methane content, production, consumption, and storage within the soil depth.

The model is calibrated with laboratory experiments and field measurements of peatland. They showed the importance of aggregate size on methane emission. Increasing mean aggregate size leads to higher methane emissions during the growing season and fall refreezing, as discussed by the authors. They also explored the impact of water table position on methane emission. Lowering the water table level and increasing the oxygenated percentage of the soil profile result in reduced net methane emissions from the soil surface, according to the model's results. This reduction is likely due to changes in the relative size and activity of methanogenic and methanotrophic microbial communities as

the water table position decreases. However, the model predicts lower methane emission amounts when simulating changes in water table position compared to field data. This discrepancy could be attributed to potential underestimation of anoxic conditions, which are necessary for methane production, or the model's failure to account for local variations in water table position that may differ from the average value utilized in the simulations.

In another study, Knoblauch et al. (2021) has developed a model to measure greenhouse gas emissions from permafrost which is based on field measurement. During two summer seasons, they measured CO_2 and CH_4 fluxes from soils affected by sudden thaw slump in permafrost, also referred to as thermokarst, in Siberia. These field observations alongside with long-term incubation data were used to calibrate two models that simulate CO_2 and CH_4 productions from microbial activity. Thermokarst are excellent environments for studying the in situ decomposition of organic matter (OM) in freshly thawed permafrost. Due to rapid erosion, the surface of the active thaw slump is free of recent vegetation, and only microbes' respiration contributes to CO_2 and CH_4 emissions at the site.

The results from this experiment have been used as input for their two-carbon-pool model. They divided the carbon pool into labile and resistant. For each pool, the following equation is used:

$$-\frac{dC}{dt} = kC \tag{50}$$

where k is the rate constant that indicates varying decomposition rates for the organic matter in each pool. A portion (fraction h) of the fast decomposing material from the labile pool moves to the slower decomposing stable pool, which represents humification. Humification is a process in which organic matter, such as plant and animal residues, decomposes and transforms into more stable forms of organic matter called humus. The rest of the material $(1-h)$ becomes trace gas and exits the system. The degradation of carbon in the stable pool is assumed to fully contribute to the trace gas emission. The starting amount of total soil organic carbon is based on observations. The initial fraction of the labile pool is considered a fixed value, and the initial fraction of the stable carbon pool is calculated as the difference from the total carbon content. Then, by using a regression method, they determined the values of decomposition rates, initial labile carbon pool fraction, and the humification coefficient. In another approach, they used Q_{10} model to calibrate their model. This calibrated model was then applied to estimate CO_2 emissions. They obtained topsoil temperatures from the JSBACH (Jena Scheme for Biosphere-Atmosphere Coupling in Hamburg) land surface scheme which is a land surface model used to simulate the exchange of energy, water, and carbon between the Earth's surface and the atmosphere. Following this approach, they developed a formula in order to estimate CO_2 and CH_4 areal fluxes as follows:

$$f_p = \sum_{i=1}^{2}\left(\rho_i \cdot d_i \cdot r_i \cdot Q_{10}^{\frac{T_i-4}{10}}\right) \tag{51}$$

where r_i $\left[\mathrm{M}^{-1}\ \mathrm{T}^{-1}\right]$ indicates aerobic or anaerobic gas production rate calculated at 4 °C in samples incubated from layer i, ρ_i $\left[\mathrm{M}\ \mathrm{L}^{-3}\right]$ is dry bulk density of soil layer, d_i is the soil layer depth, T_i [C] is the mean temperature of layer i during the field measurement day. Q_{10} is the temperature sensitivity factor.

Finally, the study estimated the annual carbon dioxide (CO_2) emissions from heterotrophic respiration in tundra soil at different thaw slump sites using two modeling approaches. The model was validated with field data. Comparing two approaches used for the calibration of the model they found that the Q_{10} model simulates CO_2 fluxes at any temperature below 0 °C, while the ICBM model simulates microbial CO_2 production only at temperatures above −10 °C. From January 1, 2016, to May 24, 2016, the simulated surface soil temperatures were below −10 °C, and the ICBM assumed zero CO_2 production during this time. This indicates the importance of calibration method in mathematical models and shows that calibrating a mathematical model is not the same as validating. As different calibration methods can lead to different results and interpretations.

7. Parameters interdependency

In this section, we conduct a comprehensive study to analyze the effective parameters in soil respiration modeling. Per reviewing the mathematical models presented in the area of soil respiration and PCF, five key factors that play important roles in developing a mathematical model are temperature, soil moisture, soil organic matter content time, and soil depth. Table 3 shows an overview of these factors based on the models reviewed.

8. Discussions and conclusion

The objective of this review paper is to emphasize the significant role of microbial activity in the context of the PCF. The main motivation is to identify research directions that can contribute to enhancing model development for accurately projecting carbon feedback associated with permafrost thaw. Thus, after having provided an overview of experimental studies, including both in situ and laboratory investigations, that demonstrate the involvement of microorganisms and plants in PCF, we then have presented different approaches used to model these complex mechanisms. In order to provide a wider range of mathematical frameworks, our review initially incorporates models of soil respiration and plant-microorganism interactions, which were originally developed outside the specific context of permafrost soil. Finally, the last section of the paper focuses on mathematical models dedicated to PCF, specifically including the influence of plants and microorganisms.

The literature review concerning the role of microorganisms and plants in PCF has revealed the complex nature of the ecosystem under consideration. Numerous physical parameters have emerged as significant factors in this process. Table 4 provides a summary of these parameters, which have been investigated over the last two decades. Soil temperature, soil unfrozen water content, soil properties (e.g. soil texture, porosity, size of the aggregates), vegetation type, soil salinity, quantity, and quality of organic matter (fast or slow carbon decomposability), as well as the types and abundance of microorganisms, are all local soil characteristics that profoundly influence the greenhouse gas emissions to the atmosphere. Additionally, the chosen spatial resolution of the model and the time scale have been shown to exhibit diverse behaviors. Noting that 10 out of 25 conducted studies have covered a duration of at least one year.

Process-based models have shown to provide an effective method for modeling soil respiration as they combine a physical description of transport mechanisms complemented with additional equations to capture complex biological processes that cannot be adequately represented by purely physical models. The challenge lies on the reliance of these models on a particular description of a specific ecosystem. Often, model parameters are calibrated based on field or laboratory measurements, limiting the effectiveness of the considered process model to only specific spatial and temporal resolutions. As an illustration, numerous respiration models are based on the deviation of carbon production from optimal conditions, typically assumed to occur at 20 degrees Celsius (Šimůnek and Suarez, 1993; Fang and Moncrieff, 1999). In these models, no respiration is considered to occur around zero degrees Celsius. Therefore, it is necessary to develop entirely new descriptions of certain processes to adapt some of these respiration models for permafrost environments. The same remarks hold true for the description of the rhizosphere priming effect, thus the modeling of plant-microorganisms interaction.

More recently, models have emerged to describe methane and carbon dioxide emissions from permafrost. However, permafrost ecosystems themselves present a significant challenge to describe due to their

Table 3
Summary of soil respiration models.

Parameter	Temperature (T)	Soil moisture (θ)	Organic carbon content ([c])	Oxygen content ([O_2])	Soil depth (z)	Soil Respiration (CO_2 emission) rate
Temperature (T)	–	In general, high temperature leads to decreasing soil moisture due to evaporation. For permafrost condition, the temperature increase leads to higher availability of liquid water.	Temperature increase can accelerate the decomposition rate and increase the availability of organic carbon.	This is directly affected by soil moisture, so, in general, increasing the temperature will lead to enhancing oxygen levels. In permafrost, thawing may lead to waterlogged conditions, causing limited oxygen availability.	Temperature increase may cause an increase in the active layer depth.	The respiration rate highly depends on temperature changes. Temperature leads to raising the respiration rate, and declining the temperature decreases it. For permafrost condition, when the temperature is below freezing point, there is a very low rate of respiration.
Soil moisture (θ)	Soil moisture can affect thermal conductivity. So, it impacts the heat conduction through the soil profile. Higher moisture content leads to higher heat conductivity.	–	It can be considered effective in very high or low moisture levels as it directly impacts microbial activity.	High moisture content creates anaerobic (low oxygen) conditions. On the other hand, in low moisture conditions, soil pores may become air-filled.	–	Soil moisture is considered a parameter effective when the moisture level is too high or too low. High moisture means anaerobic conditions and so low respiration rate. Low moisture availability means aerobic conditions and high respiration rate. However, in very low moisture conditions, or drying soil, the respiration rate may decline due to low moisture availability for microbial activity.
Oxygen content ([O_2])	Can affect the thermal conductivity of soil. Lower oxygen means higher thermal conductivity.	Soil moisture and oxygen content are highly dependent. Any changes in soil moisture content affect oxygen availability.	It can be considered effective in very high or low moisture levels as it directly impacts microbial activity and subsequently the decomposition rate.	–	–	Low oxygen availability may cause a low respiration rate but it does not always mean less carbon emission from the soil. In anoxic conditions, some kinds of microorganisms can keep their activity and release methane. This is one of the persisting drawbacks in PCF modeling.
Soil depth (z)	Temperature distribution through the soil profile changes depending on the thermal conductivity of the soil. So, the temperature changes spatially.	Moisture content changes with the soil depth. The presence of plant roots, and the uptake rate, microbial activity, and the temperature changes are the parameters that affect soil moisture content through the soil profile.	The availability of organic carbon is different in each soil layer. The depth is one of the most important parameters to be considered while modeling organic carbon content.	Oxygen content changes with soil depth, as it is directly affected by the soil moisture content.	–	
Time (t)	Temperature is a time-dependent parameter. Daily, monthly, and seasonal temperature changes can be considered through time.	As moisture content depends on the temperature, this parameter is also a time-dependent one. The soil moisture level is changing through time.	The effect of time on the concentration of organic carbon is one of the most important parameters that are challenging to consider while developing a numerical model. Usually, in the models, we have carbon pools available in which the concentration does not change with time. The spatial effect is mostly considered in the models, but time is missing.	Oxygen content changes with soil depth, as it is directly affected by the soil moisture content. Due to the direct impact of moisture on oxygen content, it is clear that oxygen content is also a time-dependent parameter. However, this is one of the gaps in most PCF models, as oxygen is not usually considered a time-dependent parameter and is considered constant.	–	Time is one of the important factors while calculating soil respiration rate. Short-term and long-term studies proved to have different results. A nice example would be a high participation rate over a period of time. If we compute the respiration rate for that period, our results will be imprecise and may lead to an incorrect conclusion.

inherent complexity. Even at the regional scale, permafrost conditions can vary greatly, with diverse characteristics ranging from permanently frozen layers to seasonally thawing layers and permanently thawed layers (i.e., taliks). Besides, when studying carbon dynamics in permafrost, it is essential to take a detailed assessment of temporal factors. The key question of whether permafrost will transition from a carbon sink to a carbon source lies on the balance of carbon fluxes over several consecutive years. The cyclical process of carbon sequestration in the soil during plant growth in spring, followed by its release through soil respiration during the plant regeneration phase in fall, plays a key role in predicting the overall net carbon feedback in permafrost ecosystems. Incorporating transport processes such as diffusion, convection, transport through plant tissues, and water flow into models becomes crucial to provide a more realistic representation of carbon dynamics and facilitate predictions under diverse climate scenarios and time frames. Furthermore, these transport mechanisms are not only relevant for describing the movement of greenhouse gases from the soil to the atmosphere but also play a critical role in regulating the availability of substrates, such as organic matter and nutrients. These substrate availability factors significantly influence microbial activity and carbon decomposition rates.

Most existing models operate under the common assumption that soil respiration measured at the surface reliably reflects the concurrent subsurface production of CO_2 by roots and microbes. However, Samuels-Crow et al. (2018) conducted an extensive study to explore the validity of this hypothesis across different time scales. Their research demonstrated that, under specific conditions of soil textures, root and microbial depth distributions, soil temperature, and soil water content, the assumption holds true at seasonal time scales. However, at subdaily to monthly time scales, variations in temporal coherence and time lags between measured soil respiration and total soil CO_2 production were observed, challenging the notion that soil respiration provides an accurate snapshot of subsurface CO_2 production. This raises questions not only about the comparison of models to field measurements but also about the appropriate construction of models regarding the treatment of carbon production and carbon transport. Soil texture, along with the associated soil water content and soil temperature profiles, emerges as a pivotal factor influencing the temporal coherence and time lags between subsurface and surface CO_2 fluxes. The complexity arises from the multitude of potential mechanisms that may come into play for each factor, making the model description either highly complex or valid only at a very regional scale. For example, some studies have attributed increased soil respiration following precipitation events to physical mechanisms, such as the displacement of CO_2 stored in dry soil pores (water flux description in (Jassal et al., 2004; Suarez and Šimůnek, 1993)) or biological mechanisms such as increased microbial activity (Keuper et al., 2020). However, soil respiration can also decrease following precipitation events, which has also been attributed to physical mechanisms such as a decreased diffusivity (Suarez and Šimůnek, 1993) and biological processes as a shift from aerobic to anaerobic decomposition (Ebrahimi and Or, 2016). Besides, soil bulk density and particle size distribution exert direct control over CO_2 diffusivity because they control pore size distribution, water retention, and air-filled and total porosity at each depth and time (Ryan et al., 2018). As a result, there will be a drop in CO_2 diffusivity in all soil types if precipitation declines and subsequently affects soil temperature profiles and soil moisture content. Due to its direct control over CO_2 diffusivity through soil bulk density and particle size distribution, which determine pore size distribution, water retention, and air-filled and total porosity at each depth and time, this impact is more noticeable in fine-grained (e.g., clay) soils.

Another significant aspect in the numerical modeling of the permafrost ecosystem is related to boundary conditions and initial conditions. In other words, the initial description of the ecosystem in terms of soil properties (e.g. soil texture, porosity, size of the aggregates, temperature), vegetation type, quantity, and quality of organic matter (fast or slow carbon decomposability), as well as the types and abundance of microorganisms should be predefined. Adding to the complexity is considering climate nonstationarity in numerical modeling of PCF. In fact, it's likely that precipitation events will grow more powerful but less frequent, with longer periods of dry weather in between storms (Zelikova et al., n.d.). In the Arctic, a change from solid (snow) to liquid precipitation (rain) is very likely, impacting surface hydrology, increasing the level of complexity. Moreover, the combination of a changing climate (for instance, hot and dry conditions) is expected to escalate the potential, frequency, and severity of wildfires in northern regions, leading to sudden and profound transformations in the affected ecosystems (Singh, n.d.) and permafrost areas.

Undoubtedly, the complex and dynamic nature of permafrost ecosystems, characterized by the convergence of physical, chemical, and biological processes, underscores the need for the construction of comprehensive thermo-hydro-biogeochemical models. Integrating multiple processes and factors within these models offers a quantitative framework to comprehend the behavior and dynamics of permafrost systems amidst evolving environmental conditions. By developing such a model, enhanced predictions, effective mitigation strategies, and informed management approaches can be achieved for permafrost regions, thereby preserving, or slowing down the degradation of, these distinctive and vulnerable ecosystems in the context of ongoing climate change. For the moment, the wide range of approaches across the different models results in a large discrepancy in the predicted carbon dynamic, which is a call for developing robust validation procedures (Le Noë et al., 2023). In this review paper, we have looked into the development of a mathematical framework to describe the contribution of microbial activity and plants to the PCF. However, we have not addressed the question of model validation, which is a critical phase of model development. By adding processes to the carbon feedback model, they are becoming increasingly complex, which might end up in hidden compensating biases arising from the overfitting of model parameters. One idea could be to use different processed-based models, with different levels of complexity, to simulate the same observation of carbon dynamics in order to identify the mathematical framework allowing the best performance.

CRediT authorship contribution statement

Niloofar Fasaeiyan: Writing – original draft, Visualization, Validation, Methodology, Investigation, Formal analysis, Data curation, Conceptualization. **Sophie Jung:** Writing – review & editing, Writing – original draft, Visualization, Validation, Methodology, Investigation, Formal analysis, Data curation, Conceptualization. **Richard Boudreault:** Writing – review & editing. **Lukas U. Arenson:** Writing – review & editing, Formal analysis. **Pooneh Maghoul:** Writing – review & editing, Writing – original draft, Validation, Supervision, Resources, Project administration, Methodology, Investigation, Funding acquisition, Formal analysis, Data curation, Conceptualization.

Declaration of competing interest

The authors declare that they have no known competing financial interests or personal relationships that could influence the work reported in this paper.

Data availability

Data will be made available on request.

Acknowledgements

The authors acknowledge the financial support of the Natural Sciences and Engineering Research Council of Canada (NSERC) (ALLRP

576419 - 22), PRIMA Québec, BGC Engineering, Object Research Systems (ORS), and Awn Nanotech.

Appendix A

Table 4
Summary of the various parameters affecting microbial activity in thawing permafrost, studied in the literature review.

Paper	Soil Temperature	Vegetation	Water Content	Soil Properties	Microbial Life	Nature of the Experiment	Carbon Feedback	Duration
Sun et al., (2023)	◇			◇		in situ	CO_2	9 years (June 2011–2020)
Dong et al., (2023)	◇				◇	Lab	/	/
Sipes et al., (2022)				◇	◇	Lab	CO_2	/
Knoblauch et al., (2021)	◇	◇				in situ	CO_2, CH_4	3 years (July 2016–2019), long-term incubation (6 months)
Yun et al., (2022)	◇		◇	◇	◇	in situ	CO_2	6 years (June 2012–October 2018)
Qin et al., (2021)	◇			◇		Lab	CO_2	Long-term (>400 days), short-term (28 days)
Song et al., (2021)	◇			◇	◇	Lab	CO_2	90 days
Meisner et al., (2021)			◇		◇	Lab	CO_2, CH_4	1 month incubation +1 week for each phase of the cycle
Monteux et al., (2020)					◇	Lab	CO_2	160 days
Peng et al., (2020)	◇				◇	in situ	CO_2	9 years
Bouskil et al., (2020)	◇	◇			◇	in situ	CO_2	10 years
Song et al., (2020)			◇			Lab	CO_2, CH_4	239 days
Li et al., (2020)	◇			◇		in situ	CO_2, CH_4	4 years
Lynch et al., (2018)		◇				in situ	CO_2	1 year (May 2014–2015)
Yang et al., (2018)	◇		◇			in situ	CH_4	2 years
Voigt et al., (2017)	◇	◇				in situ	CO_2, CH_4	2 years
Yang et al., (2017)			◇		◇	in situ	CH_4	Measurement in August 2012
Stapel et al., (2016)	◇		◇		◇	Lab	CO_2, CH_4	/
Coolen and Orsi, (2015)	◇				◇	Lab	CO_2, CH_4	/
Chowdhury et al., (2015)	◇		◇		◇	Lab	CO_2, CH_4	60 days
Shi et al., (2015)		◇			◇	Lab	/	/
Schneider Von Deimling et al., (2015)	◇		◇			in situ	CO_2, CH_4	/
Waldrop et al., (2010)	◇				◇	Lab	CO_2, CH_4	98 days aerobic treatment, 117 days anaerobic
Sturm et al., (2005)		◇	◇		◇	in situ	CO_2	/

References

Adingo, Samuel, Jie-Ru, Yu, Xue-Lu, Liu, Li, Xiaodan, Jing, Sun, Xiaong, Zhang, 2021. Variation of soil microbial carbon use efficiency (cue) and its influence mechanism in the context of global environmental change: a review. PeerJ 9 (e12131), 10.

Aqeel, Muhammad, Ran, Jinzhi, Weigang, Hu, Irshad, Muhammad Kashif, Dong, Longwei, Akram, Muhammad Adnan, Eldesoky, Gaber E., Aljuwayid, Ahmed Muteb, Chuah, Lai Fatt, Deng, Jianming, 2023. Plant-soil-microbe interactions in maintaining ecosystem stability and coordinated turnover under changing environmental conditions. Chemosphere 318, 137924.

Christian Beer, Markus Reichstein, Enrico Tomelleri, Philippe Ciais, Martin Jung, Nuno Carvalhais, Christian Rödenbeck, M. Altaf Arain, Dennis Baldocchi, Gordon B. Bonan, Alberte Bondeau, Alessandro Cescatti, Gitta Lasslop, Anders Lindroth, Mark Lomas, Sebastiaan Luyssaert, Hank Margolis, Keith W. Oleson, Olivier Roupsard, Elmar Veenendaal, Nicolas Viovy, Christopher Williams, F. Ian Woodward, and Dario Papale. Terrestrial gross carbon dioxide uptake: Global distribution and covariation with climate. 329(5993):834–838.

Bengtson, Per, Barker, Jason, Grayston, Sue J., 2012. Evidence of a strong coupling between root exudation, c and n availability, and stimulated som decomposition caused by rhizosphere priming effects. Ecol. Evol. 2 (8), 1843–1852.

Berner, Logan T., Massey, Richard, Jantz, Patrick, Forbes, Bruce C., Macias-Fauria, Marc, Myers-Smith, Isla, Kumpula, Timo, Gauthier, Gilles, Andreu-Hayles, Laia, Gaglioti, Benjamin V., et al., 2020. Summer warming explains widespread but not uniform greening in the arctic tundra biome. Nat. Commun. 11 (1), 1–12.

Biskaborn, Boris K., Smith, Sharon L., Noetzli, Jeannette, Matthes, Heidrun, Vieira, Gonçalo, Streletskiy, Dmitry A., Schoeneich, Philippe, Romanovsky, Vladimir E., Lewkowicz, Antoni G., Abramov, Andrey, et al., 2019. Permafrost is warming at a global scale. Nat. Commun. 10 (1), 264.

Bouskill, Nicholas, Riley, William, Zhu, Qing, Mekonnen, Zelalem, Grant, R.F., 2020. Alaskan carbon-climate feedbacks will be weaker than inferred from short-term experiments. Nat. Commun. 11, 11.

Burke, E.J., Chadburn, S.E., Ekici, A., 2017. A vertical representation of soil carbon in the jules land surface scheme (vn4.3_permafrost) with a focus on permafrost regions. Geosci. Model Dev. 10 (2), 959–975.

Charles Tarnocai, J.G., Canadell, Edward A.G., Schuur, Peter Kuhry, Mazhitova, G., Zimov, S., 2009. Soil organic carbon pools in the northern circumpolar permafrost region. Global Biogeochem. Cycles 23 (2).

Chertov, Oleg, Kuzyakov, Yakov, Priputina, Irina, Frolov, Pavel, Shanin, Vladimir, Grabarnik, Pavel, Oct 2022. Modelling the rhizosphere priming effect in combination with soil food webs to quantify interaction between living plant, soil biota and soil organic matter. Plants 11 (19), 2605.

Core Writing Team, 2023. In: Lee, H., Romero, J. (Eds.), Climate Change 2023: Synthesis Report. Contribution of Working Groups I, II and III to the Sixth Assessment Report of the Intergovernmental Panel on Climate Change. IPCC, Geneva, Switzerland.

Dijkstra, Feike, Carrillo, Yolima, Pendall, Elise, Morgan, Jack, 2013. Rhizosphere priming: a nutrient perspective. Front. Microbiol. 4 (216), 07.

Duchesne, Caroline, Smith, Sharon, Ednie, Mark, Bonnaventure, Philip, 2015. Active layer variability and change in the mackenzie valley, northwest territories, 09.

Ebrahimi, Ali, 2017. Mechanistic modeling of microbial interactions at pore to profile scale resolve methane emission dynamics from permafrost soil. J. Geophys. Res. Biogeo. 122, 05.

Ebrahimi, Ali N., Or, Dani, 2014. Microbial dispersal in unsaturated porous media: characteristics of motile bacterial cell motions in unsaturated angular pore networks. Water Resour. Res. 50 (9), 7406–7429.

Ebrahimi, Ali, Or, Dani, 2015. Hydration and diffusion processes shape microbial community organization and function in model soil aggregates. Water Resour. Res. 51 (12), 9804–9827.

Ebrahimi, Ali, Or, Dani, 2016. Microbial community dynamics in soil aggregates shape biogeochemical gas fluxes from soil profiles – upscaling an aggregate biophysical model. Glob. Chang. Biol. 22 (9), 3141–3156.

Elberling, Bo, Brandt, Kristian K., 2003. Uncoupling of microbial co2 production and release in frozen soil and its implications for field studies of arctic c cycling. Soil Biol. Biochem. 35 (2), 263–272.

Fang, C., Moncrieff, John B., 1999. A model for soil co2 production and transport 1: model development. Agric. For. Meteorol. 95 (4), 225–236.
Froese, Duane G., Westgate, John A., Reyes, Alberto V., Enkin, Randolph J., Preece, Shari J., September 2008. Ancient permafrost and a future, warmer arctic. Science (New York, N.Y.) 321 (5896), 1648.
Frolking, Steve, Talbot, Julie, Jones, Miriam C., Treat, Claire C., Boone Kauffman, J., Tuittila, Eeva-Stiina, Roulet, Nigel, 2011. Peatlands in the earth's 21st century climate system. Environ. Rev. 19 (NA), 371–396.
Geyer, Kevin, Kyker-Snowman, Emily, Grandy, Stuart, Frey, Serita, 2016. Microbial carbon use efficiency: accounting for population, community, and ecosystem-scale controls over the fate of metabolized organic matter. Biogeochemistry 127, 02.
Gruber, S., 2020. Ground subsidence and heave over permafrost: hourly time series reveal interannual, seasonal and shorter-term movement caused by freezing, thawing and water movement. Cryosphere 14 (4), 1437–1447.
Hicks Pries, Caitlin E., Schuur, Edward A.G., Crummer, Kathryn G., 2013. Thawing permafrost increases old soil and autotrophic respiration in tundra: partitioning ecosystem respiration using δ13c and 14c. Glob. Chang. Biol. 19 (2), 649–661.
Hollesen, J., Elberling, B., Jansson, P.E., 2011. Future active layer dynamics and carbon dioxide production from thawing permafrost layers in northeast greenland. Glob. Chang. Biol. 17 (2), 911–926.
Holloway, Jean E., Lewkowicz, Antoni G., Douglas, Thomas A., Li, Xiaoying, Turetsky, Merritt R., Baltzer, Jennifer L., Jin, Huijun, 2020. Impact of wildfire on permafrost landscapes: a review of recent advances and future prospects. Permafr. Periglac. Process. 31 (3), 371–382.
Homer-Dixon, Thomas, Froese, Duane, 2021. Canada's thawing permafrost should be raising alarm bells in the battle against climate change. GLOBE AND MAI.
Hugelius, Gustaf, Strauss, Jens, Zubrzycki, Sebastian, Harden, Jennifer W., Schuur, Edward A.G., Ping, C.-L., Schirrmeister, Lutz, Grosse, Guido, Michaelson, Gary J., Koven, Charles D., et al., 2014. Estimated stocks of circumpolar permafrost carbon with quantified uncertainty ranges and identified data gaps. Biogeosciences 11 (23), 6573–6593.
Hugelius, Gustaf, Loisel, Julie, Chadburn, Sarah, Jackson, Robert B., Jones, Miriam, MacDonald, Glen, Marushchak, Maija, Olefeldt, David, Packalen, Maara, Siewert, Matthias B., Treat, Claire, Turetsky, Merritt, Voigt, Carolina, Zicheng, Yu., 2020. Large stocks of peatland carbon and nitrogen are vulnerable to permafrost thaw. Proc. Natl. Acad. Sci. 117 (34), 20438–20446.
Isaksen, Ketil, Nordli, Øyvind, Ivanov, Boris, Køltzow, Morten A.Ø., Aaboe, Signe, Gjelten, Herdis M., Mezghani, Abdelkader, Eastwood, Steinar, Førland, Eirik, Benestad, Rasmus E., et al., 2022. Exceptional warming over the barents area. Sci. Rep. 12 (1), 1–18.
Jackson, Oyindamola, Quilliam, Richard, Stott, Andy, Grant, Helen, Subke, Jens-Arne, 2019. Rhizosphere carbon supply accelerates soil organic matter decomposition in the presence of fresh organic substrates. Plant and Soil 440, 07.
Jassal, R.S., Black, T.A., Drewitt, G.B., Novak, M.D., Gaumont-Guay, D., Nesic, Z., 2004. A model of the production and transport of co2 in soil: predicting soil co2 concentrations and co2 efflux from a forest floor. Agric. For. Meteorol. 124 (3–4), 219–236.
Keuper, Frida, Wild, Birgit, Kummu, Matti, Beer, Christian, Blume-Werry, Gesche, Fontaine, Sébastien, Gavazov, Konstantin, Gentsch, Norman, Guggenberger, Georg, Hugelius, Gustaf, et al., 2020. Carbon loss from northern circumpolar permafrost soils amplified by rhizosphere priming. Nat. Geosci. 13 (8), 560–565.
Knoblauch, Christian, Beer, Christian, Schuett, Alexander, Sauerland, Lewis, Liebner, Susanne, Steinhof, Axel, Rethemeyer, Janet, Grigoriev, Mikhail N., Faguet, Alexey, Pfeiffer, Eva-Maria, 2021. Carbon dioxide and methane release following abrupt thaw of pleistocene permafrost deposits in arctic siberia. J. Geophys. Res. Biogeosci. 126 (11), e2021JG006543 e2021JG006543 2021JG006543.
Koven, Charles D., Ringeval, Bruno, Friedlingstein, Pierre, Ciais, Philippe, Cadule, Patricia, Khvorostyanov, Dmitry, Krinner, Gerhard, Tarnocai, Charles, 2011. Permafrost carbon-climate feedbacks accelerate global warming. Proc. Natl. Acad. Sci. 108 (36), 14769–14774.
Koven, Charles D., Riley, William J., Stern, Alex, 2013. Analysis of permafrost thermal dynamics and response to climate change in the cmip5 earth system models. J. Climate 26 (6), 1877–1900.
Koven, Charles D., Lawrence, David M., Riley, William J., 2015. Permafrost carbon-climate feedback is sensitive to deep soil carbon decomposability but not deep soil nitrogen dynamics. Proc. Natl. Acad. Sci. 112 (12), 3752–3757.
Kuklina, Vera, Oleg, Sizov, Rasputina, Elena, Krasnoshtanova, Natalia, Bogdanov, Victor, Bilichenko, Irina, Petrov, Andrey, 2022. Fires on ice: emerging permafrost peatlands fire regimes in russia's subarctic taiga. Land 11 (322), 02.
Kuzyakov, Yakov, Horwath, William R., Dorodnikov, Maxim, Blagodatskaya, Evgenia, 2018. Chapter eight - effects of elevated co2 in the atmosphere on soil c and n turnover. In: Horwath, William R., Kuzyakov, Yakov (Eds.), Climate Change Impacts on Soil Processes and Ecosystem Properties, vol. 35. Elsevier, pp. 207–219 of *Developments in Soil Science*,.
Lawrence, David M., Slater, Andrew G., Romanovsky, Vladimir E., Nicolsky, Dmitry J., 2008. Sensitivity of a model projection of near-surface permafrost degradation to soil column depth and representation of soil organic matter, 113, F02011.
Lawrence, David, Slater, Andrew, Swenson, Sean, 2012. Simulation of present-day and future permafrost and seasonally frozen ground conditions in ccsm4. J. Climate 25 (04), 2207–2225.
Le Noë, Julia, Manzoni, Stefano, Abramoff, Rose, Bölscher, Tobias, Bruni, Elisa, Cardinael, Rémi, Ciais, Philippe, Chenu, Claire, Clivot, Hugues, Derrien, Delphine, et al., 2023. Soil organic carbon models need independent time-series validation for reliable prediction. Commun. Earth Environ. 4 (1), 158.
Lewkowicz, Antoni G., Way, Robert G., 2019. Extremes of summer climate trigger thousands of thermokarst landslides in a high arctic environment. Nat. Commun. 10 (1), 1–11.
Li, Xiaoying, Jin, Huijun, Wang, Hong-Wei, Marchenko, Sergey, Shan, Wei, Luo, Dongliang, He, Ruixia, Spektor, Valentin, Huang, Ya-Dong, Li, Xin-Yu, Jia, Ning, 2021. Influences of forest fires on the permafrost environment: a review. Adv. Clim. Chang. Res. 12, 01.
Liu, Hongwei, Maghoul, Pooneh, Shalaby, Ahmed, Bahari, Ako, 2019. Thermo-hydro-mechanical modeling of frost heave using the theory of poroelasticity for frost-susceptible soils in double-barrel culvert sites. Transp. Geotech. 20, 100251.
Liu, Zhihua, Kimball, John S., Ballantyne, Ashley, Watts, Jennifer D., Natali, Susan M., Rogers, Brendan M., Yi, Yonghong, Klene, Anna E., Moghaddam, Mahta, Jinyang, Du, Zona, Donatella, dec 2023. Widespread deepening of the active layer in northern permafrost regions from 2003 to 2020. Environ. Res. Lett. 19 (1), 014020.
Luke, C.M., Cox, P.M., 2011. Soil carbon and climate change: from the jenkinson effect to the compost-bomb instability. Eur. J. Soil Sci. 62 (1), 5–12.
Lulham, N., Warren, F.J., Walsh, K.A., Szwarc, J., 2023. Canada in a Changing Climate: Synthesis Report. Natural Resources Canada. Open Access.
Magnin, F., Josnin, J.-Y., 2021. Water flows in rock wall permafrost : a numerical approach coupling hydrological and thermal processes. J. Geophys. Res. Earth 126, 1–20.
Mahecha, Miguel D., Reichstein, Markus, Carvalhais, Nuno, Lasslop, Gitta, Lange, Holger, Seneviratne, Sonia I., Vargas, Rodrigo, Christof Ammann, M., Arain, Altaf, Cescatti, Alessandro, Janssens, Ivan A., Migliavacca, Mirco, Montagnani, Leonardo, Richardson, Andrew D., 2010. Global convergence in the temperature sensitivity of respiration at ecosystem level. Science 329 (5993), 838–840.
McGuire, A.D., Christensen, T.R., Hayes, D., Heroult, A., Euskirchen, E., Kimball, J.S., Koven, C., Lafleur, P., Miller, P.A., Oechel, W., Peylin, P., Williams, M., Yi, Y., 2012. An assessment of the carbon balance of arctic tundra: comparisons among observations, process models, and atmospheric inversions. Biogeosciences 9 (8), 3185–3204.
McGuire, A. David, Lawrence, David M., Koven, Charles, Clein, Joy S., Burke, Eleanor, Chen, Guangsheng, Jafarov, Elchin, MacDougall, Andrew H., Marchenko, Sergey, Nicolsky, Dmitry, Peng, Shushi, Rinke, Annette, Ciais, Philippe, Gouttevin, Isabelle, Hayes, Daniel J., Ji, Duoying, Krinner, Gerhard, Moore, John C., Romanovsky, Vladimir, Schädel, Christina, Schaefer, Kevin, Schuur, Edward A.G., Zhuang, Qianlai, 2018. Dependence of the evolution of carbon dynamics in the northern permafrost region on the trajectory of climate change. Proc. Natl. Acad. Sci. 115 (15), 3882–3887.
A. David McGuire, Charles Koven, David M. Lawrence, Joy S. Clein, Jiangyang Xia, Christian Beer, Eleanor Burke, Guangsheng Chen, Xiaodong Chen, Christine Delire, Elchin Jafarov, Andrew H. MacDougall, Sergey Marchenko, Dmitry Nicolsky, Shushi Peng, Annette Rinke, Kazuyuki Saito, Wenxin Zhang, Ramdane Alkama, Theodore J. Bohn, Philippe Ciais, Bertrand Decharme, Altug Ekici, Isabelle Gouttevin, Tomohiro Hajima, Daniel J. Hayes, Duoying Ji, Gerhard Krinner, Dennis P. Lettenmaier, Yiqi Luo, Paul A. Miller, John C. Moore, Vladimir Romanovsky, Christina Schädel, Kevin Schaefer, Edward A.G. Schuur, Benjamin Smith, Tetsuo Sueyoshi, and Qianlai Zhuang. Variability in the sensitivity among model simulations of permafrost and carbon dynamics in the permafrost region between 1960 and 2009: Model. Permafr. Carbon Dyn.. 30(7):1015–1037.
Meinshausen, Malte, Raper, Sarah C.B., Wigley, Tom M.L., 2011. Emulating coupled atmosphere-ocean and carbon cycle models with a simpler model, magicc6–part 1: model description and calibration. Atmos. Chem. Phys. 11 (4), 1417–1456.
Meisner, Annelein, Snoek, Basten L., Nesme, Joseph, Dent, Elizabeth, Jacquiod, Samuel, Classen, Aimée T., Priemé, Anders, 2021. Soil microbial legacies differ following drying-rewetting and freezing-thawing cycles. ISME J. 15 (4), 1207–1221.
Mishra, Umakant, Hugelius, Gustaf, Shelef, Eitan, Yang, Yuanhe, Strauss, Jens, Lupachev, Alexey, Harden, Jennifer W., Jastrow, Julie D., Ping, Chien-Lu, Riley, William J., et al., 2021. Spatial heterogeneity and environmental predictors of permafrost region soil organic carbon stocks. Sci. Adv. 7 (9), eaaz5236.
Monson, Russell K., Lipson, David L., Burns, Sean P., Turnipseed, Andrew A., Delany, Anthony C., Williams, Mark W., Schmidt, Steven K., 2006. Winter forest soil respiration controlled by climate and microbial community composition. Nature 439 (7077), 711–714.
Monteux, Sylvain, Keuper, Frida, Fontaine, Sébastien, Gavazov, Konstantin, Hallin, Sara, Juhanson, Jaanis, Krab, Eveline J., Revaillot, Sandrine, Verbruggen, Erik, Walz, Josefine, et al., 2020. Carbon and nitrogen cycling in yedoma permafrost controlled by microbial functional limitations. Nat. Geosci. 13 (12), 794–798.
Rhizosphere priming effects on soil carbon and nitrogen dynamics among tree species with and without intraspecific competition. New Phytol. 218 (3), 2018, 1036–1048.
Nikrad, Mrinalini P., Kerkhof, Lee J., Häggblom, Max M., 2016. The subzero microbiome: microbial activity in frozen and thawing soils. FEMS Microbiol. Ecol. 92 (6), fiw081.
Nottingham, Andrew T., Bååth, Erland, Reischke, Stephanie, Salinas, Norma, Meir, Patrick, 2019. Adaptation of soil microbial growth to temperature: using a tropical elevation gradient to predict future changes. Glob. Chang. Biol. 25 (3), 827–838.
Palmtag, Juri, Obu, Jaroslav, Kuhry, Peter, Richter, Andreas, Siewert, Matthias B., Weiss, Niels, Westermann, Sebastian, Hugelius, Gustaf, 2022. A high spatial resolution soil carbon and nitrogen dataset for the northern permafrost region based on circumpolar land cover upscaling, 14 (9), 4095–4110.
Pendall, E., Del Grosso, S., King, J.Y., LeCain, D.R., Milchunas, D.G., Morgan, J.A., Mosier, A.R., Ojima, D.S., Parton, W.A., Tans, P.P., White, J.W.C., 2003. Elevated atmospheric co2 effects and soil water feedbacks on soil respiration components in a colorado grassland. Global Biogeochem. Cycles 17 (2).

Peng, Fei, Zhang, Wenjuan, Li, Chengyang, Lai, Chimin, Zhou, Jun, Xue, Xian, Tsunekawa, Atsushi, 2020. Sustained increase in soil respiration after nine years of warming in an alpine meadow on the tibetan plateau. Geoderma 379, 114641.
Qian, Haifeng, Joseph, Renu, Zeng, Ning, 2010. Enhanced terrestrial carbon uptake in the northern high latitudes in the 21st century from the coupled carbon cycle climate model intercomparison project model projections, 16 (2), 641–656.
Qin, Shuqi, Kou, Dan, Mao, Chao, Chen, Yongliang, Chen, Leiyi, Yang, Yuanhe, 2021. Temperature sensitivity of permafrost carbon release mediated by mineral and microbial properties. Sci. Adv. 7 (32), eabe3596.
Reyes, Francisco R., Lougheed, Vanessa L., 2015. Rapid nutrient release from permafrost thaw in arctic aquatic ecosystems. Arct. Antarct. Alp. Res. 47 (1), 35–48.
Rossi, Mara, Dal Cin, Michela, Picotti, Stefano, Gei, Davide, Isaev, Vladislav S., Pogorelov, Andrey V., Gorshkov, Eugene I., Sergeev, Dmitrii O., Kotov, Pavel I., Giorgi, Massimo, Rainone, Mario L., 2022. Active layer and permafrost investigations using geophysical and geocryological methods—a case study of the khanovey area, near vorkuta, in the ne european russian arctic. Front. Earth Sci. 10.
Runge, Alexandra, Nitze, Ingmar, Grosse, Guido, 2022. Remote sensing annual dynamics of rapid permafrost thaw disturbances with landtrendr. Remote Sens. Environ. 268 (112752), 01.
Ryan, E.M., Ogle, K., Kropp, H., Samuels-Crow, K.E., Carrillo, Y., Pendall, E., 2018. Modeling soil co_2 production and transport with dynamic source and diffusion terms: testing the steady-state assumption using detect v1.0. Geosci. Model Dev. 11 (5), 1909–1928.
Samuels-Crow, Kimberly E., Ryan, Edmund, Pendall, Elise, Ogle, Kiona, 2018. Temporal coupling of subsurface and surface soil co2 fluxes: insights from a nonsteady state model and cross-wavelet coherence analysis. J. Geophys. Res. Biogeo. 123 (4), 1406–1424.
Schädel, Christina, Bader, Martin K.-F., Schuur, Edward A.G., Biasi, Christina, Bracho, Rosvel, Čapek, Petr, De Baets, Sarah, Diáková, Kateřina, Ernakovich, Jessica, Estop-Aragones, Cristian, et al., 2016. Potential carbon emissions dominated by carbon dioxide from thawed permafrost soils. Nat. Clim. Chang. 6 (10), 950–953.
Schneider von Deimling, T., Grosse, G., Strauss, J., Schirrmeister, L., Morgenstern, A., Schaphoff, S., Meinshausen, M., Boike, J., 2015. Observation-based modelling of permafrost carbon fluxes with accounting for deep carbon deposits and thermokarst activity. Biogeosciences 12 (11), 3469–3488.
Schuur, T., 2019. Permafrost and the global carbon cycle. Arctic Rep. Card 2019, 58.
Schuur, Edward A.G., Abbott, Benjamin, 2011. High risk of permafrost thaw. Nature 480 (7375), 32–33.
Schuur, Edward A.G., Bockheim, James, Canadell, Josep G., Euskirchen, Eugenie, Field, Christopher B., Goryachkin, Sergey V., Hagemann, Stefan, Kuhry, Peter, Lafleur, Peter M., Lee, Hanna, et al., 2008. Vulnerability of permafrost carbon to climate change: implications for the global carbon cycle. BioScience 58 (8), 701–714.
Schuur, Edward A.G., Abbott, B.W., Bowden, W.B., Victor Brovkin, P., Camill, J.G. Canadell, Chanton, J.P., Chapin, F.S., Christensen, T.R., Ciais, Pl, et al., 2013. Expert assessment of vulnerability of permafrost carbon to climate change. Clim. Change 119 (2), 359–374.
Schuur, Edward A.G., David McGuire, A., Schädel, Christina, Grosse, Guido, Harden, Jennifer W., Hayes, Daniel J., Hugelius, Gustaf, Koven, Charles D., Kuhry, Peter, Lawrence, David M., et al., 2015. Climate change and the permafrost carbon feedback. Nature 520 (7546), 171–179.
Schuur, Edward A.G., Abbott, Benjamin W., Commane, Roisin, Ernakovich, Jessica, Euskirchen, Eugenie, Hugelius, Gustaf, Grosse, Guido, Jones, Miriam, Koven, Charlie, Leshyk, Victor, Lawrence, David, Loranty, Michael M., Mauritz, Marguerite, Olefeldt, David, Natali, Susan, Rodenhizer, Heidi, Salmon, Verity, Schädel, Christina, Strauss, Jens, Treat, Claire, Turetsky, Merritt, 2022. Permafrost and climate change: carbon cycle feedbacks from the warming arctic. Annu. Rev. Env. Resour. 47 (1), 343–371.
Segal, Rebecca A., Lantz, Trevor C., Kokelj, Steven V., mar 2016. Acceleration of thaw slump activity in glaciated landscapes of the western canadian arctic. Environ. Res. Lett. 11 (3), 034025.
Shogren, Arial J., Zarnetske, Jay P., Abbott, Benjamin W., Iannucci, Frances, Frei, Rebecca J., Griffin, Natasha A., Bowden, William B., 2019. Revealing biogeochemical signatures of arctic landscapes with river chemistry. Sci. Rep. 9 (1), 1–11.
Šimůnek, Jiří, Suarez, Donald L., 1993. Modeling of carbon dioxide transport and production in soil: 1. Model development. Water Resour. Res. 29 (2), 487–497.
Swati Singh. "forest fire emissions: a contribution to global climate change". 5:925480.
Singh, Sangeeta, Bhoi, Tanmaya Kumar, Khan, Ifrah, Vipula Vyas, R., Athulya, Atiraj Rathi, Samal, Ipsita, 2023. Climate change drivers and soil microbe-plant interactions. In: Climate Change and Microbiome Dynamics: Carbon Cycle Feedbacks. Springer, pp. 157–176.
Slater, Andrew G., Lawrence, David M., 2013. Diagnosing present and future permafrost from climate models. J. Climate 26 (15), 5608–5623.
Song, Xiaoyan, Wang, Genxu, Ran, Fei, Huang, Kewei, Sun, Juying, Song, Chunlin, 2020. Soil moisture as a key factor in carbon release from thawing permafrost in a boreal forest. Geoderma 357, 113975.
Stapel, Janina Gabriele, Schirrmeister, Lutz, Overduin, Pier Paul, Wetterich, Sebastian, Strauss, Jens, Horsfield, Brian, Mangelsdorf, Kai, 2016. Microbial lipid signatures and substrate potential of organic matter in permafrost deposits: implications for future greenhouse gas production. J. Geophys. Res. Biogeosci. 121 (10), 2652–2666.
Stark, Sari, Kumar, Manoj, Myrsky, Eero, Vuorinen, Jere, Kantola, Anu M., Telkki, Ville-Veikko, Sjögersten, Sofie, Olofsson, Johan, Männistö, Minna K., 2023. Decreased soil microbial nitrogen under vegetation 'shrubification' in the subarctic forest–tundra ecotone: the potential role of increasing nutrient competition between plants and soil microorganisms. Ecosystems 1–20.
Lena Ström, Mikhail Mastepanov, and Torben R. Christensen. Species-specific effects of vascular plants on carbon turnover and methane emissions from wetlands. 75(1): 65–82.
Sturm, Matthew, Schimel, Josh, Michaelson, Gary, Welker, Jeffrey M., Oberbauer, Steven F., Liston, Glen E., Fahnestock, Jace, Romanovsky, Vladimir E., 2005. Winter biological processes could help convert arctic tundra to shrubland. Bioscience 55 (1), 17–26.
Suarez, Donald L., Šimůnek, Jiří, 1993. Modeling of carbon dioxide transport and production in soil: 2. Parameter selection, sensitivity analysis, and comparison of model predictions to field data. Water Resour. Res. 29 (2), 499–513.
Todd-Brown, Katherine E.O., Hopkins, Francesca M., Kivlin, Stephanie N., Talbot, Jennifer M., Allison, Steven D., 2012. A framework for representing microbial decomposition in coupled climate models. Biogeochemistry 109 (1), 19–33.
Torre Jorgenson, M., Racine, Charles H., Walters, James C., Osterkamp, Thomas E., 2001. Permafrost degradation and ecological changes associated with a warmingclimate in central alaska. Clim. Change 48 (4), 551–579.
Vaks, A., Mason, A.J., Breitenbach, S.F.M., Kononov, A.M., Osinzev, A.V., Rosensaft, M., Borshevsky, A., Gutareva, O.S., Henderson, G.M., 2020. Palaeoclimate evidence of vulnerable permafrost during times of low sea ice. Nature 577 (7789), 221–225.
Vonk, Jorien E., Tank, S.E., Walvoord, Michelle Ann, 2019. Integrating hydrology and biogeochemistry across frozen landscapes. Nat. Commun. 10 (1), 1–4.
Wang, Taihua, Yang, Dawen, Yang, Yuting, Piao, Shilong, Li, Xin, Cheng, Guodong, Bojie, Fu., 2020. Permafrost thawing puts the frozen carbon at risk over the tibetan plateau. Sci. Adv. 6 (19), eaaz3513.
Wania, R., Ross, I., Prentice, I.C., 2010. Implementation and evaluation of a new methane model within a dynamic global vegetation model: Lpj-whyme v1.3.1. Geosci. Model Dev. 3 (2), 565–584.
Sachio Yamamoto, James B. Alcauskas, and Thomas E. Crozier. Solubility of methane in distilled water and seawater. 21(1):78–80.
Yang, Guibiao, Peng, Yunfeng, Olefeldt, David, Chen, Yongliang, Wang, Guanqin, Li, Fei, Zhang, Dianye, Wang, Jun, Jianchun, Yu, Liu, Li, et al., 2018. Changes in methane flux along a permafrost thaw sequence on the tibetan plateau. Environ. Sci. Technol. 52 (3), 1244–1252.
Yun, Jeongeun, Jung, Ji Young, Kwon, Min Jung, Seo, Juyoung, Nam, Sungjin, Lee, Yoo Kyung, Kang, Hojeong, 2022. Temporal variations rather than long-term warming control extracellular enzyme activities and microbial community structures in the high arctic soil. Microb. Ecol. 1–14.
Tamara J. Zelikova, David G. Williams, Rhonda Hoenigman, Dana M. Blumenthal, Jack A. Morgan, and Elise Pendall. Seasonality of soil moisture mediates responses of ecosystem phenology to elevated CO_2 and warming in a semi-arid grassland. 103(5): 1119-1130.